

# Computing oscillatory solutions of the Euler system via $\mathcal{K}$ -convergence

Eduard Feireisl<sup>\*,♣</sup>Mária Lukáčová – Medviďová<sup>♠</sup>Bangwei She<sup>\*</sup>Yue Wang<sup>◇</sup>

\* Institute of Mathematics of the Czech Academy of Sciences  
 Žitná 25, CZ-115 67 Praha 1, Czech Republic  
 feireisl@math.cas.cz, she@math.cas.cz

♣ Institute of Mathematics, TU Berlin  
 Strasse des 17. Juni, Berlin, Germany

♠ Institute of Mathematics, Johannes Gutenberg-University Mainz  
 Staudingerweg 9, 55 128 Mainz, Germany  
 lukacova@uni-mainz.de

◇ Institute of Applied Physics and Computational Mathematics  
 Fenghao East road 2, Haidian, Beijing, China  
 wang\_yue@iapcm.ac.cn

## Abstract

We develop a method to compute effectively the Young measures associated to sequences of numerical solutions of the compressible Euler system. Our approach is based on the concept of  $\mathcal{K}$ -convergence adapted to sequences of parametrized measures. The convergence is strong in space and time (a.e. pointwise or in certain  $L^q$  spaces) whereas the measures converge narrowly or in the Wasserstein distance to the corresponding limit.

**Keywords:** Young measure, dissipative solutions,  $\mathcal{K}$ -convergence, compressible Euler system, Wasserstein distance, finite volume methods, consistent approximate solutions

---

\*The research of E.F. and B.S. leading to these results has received funding from the Czech Sciences Foundation (GAČR), Grant Agreement 18–05974S. The Institute of Mathematics of the Czech Academy of Sciences is supported by RVO:67985840.

♠M.L. has been funded by the Deutsche Forschungsgemeinschaft (DFG, German Research Foundation) - Project number 233630050 - TRR 146 as well as by TRR 165 Waves to Weather.

◇Y.W. acknowledges the support provided by President Foundation of CAEP(YZJJLX2016009).

This research has been also partially supported by the Sino-German Center funded by the Deutsche Forschungsgemeinschaft and National Natural Science Foundation of China. M.L. and B.S. would like to thank Jiequan Li and Beijing Institute of Applied Physics and Computational Mathematics for their hospitality.

# Contents

<b>1</b>	<b>Introduction</b>	<b>2</b>
<b>2</b>	<b>Approximate solutions</b>	<b>5</b>
<b>3</b>	<b>Strong vs. weak convergence</b>	<b>7</b>
3.1	Strong (pointwise) convergence . . . . .	8
3.2	Weak convergence . . . . .	9
<b>4</b>	<b><math>\mathcal{K}</math>-convergence of Young measures</b>	<b>12</b>
4.1	Strong convergence in the Wasserstein distance . . . . .	14
4.2	Convergence in first variation . . . . .	16
<b>5</b>	<b>Finite volume methods</b>	<b>17</b>
5.1	FLM finite volume method . . . . .	17
5.1.1	Stability and consistency . . . . .	20
5.2	GRP finite volume method . . . . .	21
5.3	Numerical experiments . . . . .	22
<b>6</b>	<b>Conclusion</b>	<b>31</b>

## 1 Introduction

The initial–boundary value problems to certain systems of nonlinear conservation laws are ill-posed in the class of weak solutions. An iconic example is the *Euler system* describing the time evolution of the density  $\varrho = \varrho(t, x)$ , the momentum  $\mathbf{m} = \mathbf{m}(t, x)$ , and the energy  $E = E(t, x)$  of a compressible inviscid fluid:

$$\begin{aligned}
 \partial_t \varrho + \operatorname{div}_x \mathbf{m} &= 0, \\
 \partial_t \mathbf{m} + \operatorname{div}_x \left( \frac{\mathbf{m} \otimes \mathbf{m}}{\varrho} \right) + \nabla_x p &= 0, \\
 \partial_t E + \operatorname{div}_x \left[ (E + p) \frac{\mathbf{m}}{\varrho} \right] &= 0.
 \end{aligned}
 \tag{1.1}$$

Here,  $p$  is the pressure related to  $\varrho, \mathbf{m}, E$  through a suitable equation of state. The fluid is confined to a spatial domain  $\Omega \subset \mathbb{R}^d$ ,  $d = 1, 2, 3$ , on the boundary of which we impose the impermeability condition

$$\mathbf{m} \cdot \mathbf{n}|_{\partial\Omega} = 0.
 \tag{1.2}$$

The initial state of the system is given through initial conditions

$$\varrho(0, \cdot) = \varrho_0, \quad \mathbf{m}(0, \cdot) = \mathbf{m}_0, \quad E(0, \cdot) = E_0.
 \tag{1.3}$$

The first numerical evidence that indicated ill-posedness of the Euler system was presented by Elling [21]. As proved later rigorously [14–17, 19, 27], the initial–boundary value problem (1.1)–(1.3) admits infinitely many weak solutions on a given time interval  $(0, T)$  for a rather vast class of initial data. Moreover, these solutions obey the standard entropy admissibility condition

$$\partial_t S + \operatorname{div}_x \left( S \frac{\mathbf{m}}{\varrho} \right) \geq 0, \quad (1.4)$$

where  $S$  is the total entropy of the system.

The ill-posedness of the Euler system is intimately related to the lack of compactness of the set of functions satisfying (1.1) and (1.4). Indeed bounded sequences of solutions may develop uncontrollable oscillations and/or concentrations. This phenomenon is then naturally inherited by their numerical approximations, see e.g. Fjordholm, Mishra, and Tadmor [30, 31]. This fact motivated the renewed interest in the measure-valued (MV) solutions introduced in the context of the incompressible Euler system by DiPerna and Majda [20]. The exact values of physical densities and fluxes, originally numerical functions of the physical variables  $(t, x)$ , are replaced by a family of *probability measures* (Young measure)

$$(t, x) \mapsto \mathcal{V}_{t,x} \in \mathcal{P}([\varrho, \mathbf{m}, S, E] \in R^{d+3}).$$

The values of the observable fields  $[\varrho, \mathbf{m}, S, E]$  are interpreted as the expected values:

$$\varrho(t, x) = \langle \mathcal{V}_{t,x}; \tilde{\varrho} \rangle, \quad \mathbf{m}(t, x) = \langle \mathcal{V}_{t,x}; \tilde{\mathbf{m}} \rangle, \quad S(t, x) = \langle \mathcal{V}_{t,x}; \tilde{S} \rangle, \quad E(t, x) = \langle \mathcal{V}_{t,x}; \tilde{E} \rangle.$$

In view of the observed fact that certain numerical schemes fail to provide convergent sequences of approximate solutions, Fjordholm et al. [30, 31] proposed a way how to compute the associated Young measure. Note that, in the context of numerical simulations, the convergence towards the limit (exact) solution is required to be pointwise (a.e.). On the other hand, however, the theoretical studies available so far in the literature, see e.g. [30, 31], provide only weak-(\*) convergence in  $(t, x)$ . This is of little practical interest as wildly oscillating output data are difficult to analyze in such a way.

In the present paper, we propose a new method to compute the Young measures associated to sequences of numerical solutions based on the concept of  $\mathcal{K}$ -convergence. We start by showing a remarkable property of the Euler system (1.1) that can be roughly stated as follows: either a consistent numerical approximation converges strongly (pointwise a.e.) or its (weak) limit *is not* a weak solution of the Euler system, see Section 3. In the context of numerical analysis, this property might be seen as a sharp version of the well-known *Lax-Wendroff theorem*. In view of these facts, the concept of measure-valued or other kind of generalized solution is necessary whenever the approximate sequence exhibits oscillations.

Following Balder [1], we associate to an approximate sequence  $\{\varrho_h, \mathbf{m}_h, S_h, E_h\}_{h \searrow 0}$  the Young measure

$$\mathcal{V}_{t,x}^h = \delta_{[\varrho_h(t,x), \mathbf{m}_h(t,x), S_h, E_h(t,x)]},$$

where  $\delta_Y$  is the Dirac mass concentrated at  $Y$ . As already pointed out, *observable* limits of  $\mathcal{V}_{t,x}^h$  for  $h \rightarrow 0$  must be given in terms of pointwise convergence. Unfortunately, the standard basic result of the theory of Young measures, see, e.g., Ball [3] or Pedregal [47], provides only the weak-(\*) convergence (up to a suitable subsequence):

$$\mathcal{V}^h \rightarrow \mathcal{V} \text{ weakly-(*) in } L^\infty(Q; \mathcal{P}(R^{d+3})), \quad Q \equiv (0, T) \times \Omega. \quad (1.5)$$

Thus, similarly to the approximate solutions  $[\varrho_h, \mathbf{m}_h, S_h, E_h]$ , the family  $\{\mathcal{V}^h\}_{h \searrow 0}$  may exhibit oscillations with respect to the physical space  $Q$ . From the practical point of view, therefore, the piece of information provided by the convergence (1.5) is negligible.

The concept of  $\mathcal{K}$ -convergence, developed in the framework of Young measures by Balder [1, 2], converts the weak-(\*) convergence to the desired pointwise one by replacing sequences by (suitable) Cesàro averages in the spirit of the original work by Komlós [39]:

*A sequence  $\{f_h\}_{h \searrow 0}$  of functions uniformly bounded in  $L^1$  contains a subsequence  $\{f_{h'}\}_{h' \searrow 0}$  such that*

$$\frac{1}{N} \sum_{n=1}^N f_{h'_n} \rightarrow f \text{ a.e. as } N \rightarrow \infty.$$

*Any further subsequence of  $\{f_{h'}\}$  enjoys the same property.*

Rephrased in terms of sequences of probability measures, Balder [2] obtained a remarkable extension of the Prokhorov theorem:

*If a parametrized family of probability measures  $\{\mathcal{V}_{t,x}^h\}_{h>0}$  is tight, meaning,*

$$\frac{1}{|Q|} \int_Q \mathcal{V}_{t,x}^h \, dx \, dt \text{ is tight,}$$

*then, for a suitable subsequence,*

$$\frac{1}{N} \sum_{n=1}^N \mathcal{V}_{t,x}^{h_n} \rightarrow \mathcal{V}_{t,x} \text{ narrowly in } \mathcal{P}(R^{d+3}) \text{ as } N \rightarrow \infty \text{ for a.e. } (t, x) \in Q. \quad (1.6)$$

We recall that a sequence of probability measures  $\{\mathcal{V}_n\}_{n=1}^\infty$  *converges narrowly* to a probability measure  $\mathcal{V}$  if

$$\langle \mathcal{V}_n; g \rangle \rightarrow \langle \mathcal{V}; g \rangle \quad \text{as } n \rightarrow \infty \text{ for any } g \in BC(R^{d+3}).$$

Here the symbol  $BC(R^{d+3})$  denotes the set of bounded continuous functions.

The aim of the present paper is to apply these ideas to sequences of numerical solutions of the Euler system (1.1)–(1.3). In addition to (1.6), we show that the available stability estimates yield convergence in the standard Wasserstein metric

$$W_1 \left( \frac{1}{N} \sum_{n=1}^N \mathcal{V}_{t,x}^{h_n}; \mathcal{V}_{t,x} \right) \rightarrow 0 \text{ as } N \rightarrow \infty \text{ for a.a. } (t, x) \in Q. \quad (1.7)$$

Recall that the Wasserstein distance of  $q$ -th order of probability measures  $\mathcal{N}, \mathcal{V}$  is defined as

$$W_q(\mathcal{N}, \mathcal{V}) := \left\{ \inf_{\pi \in \Pi(\mathcal{N}, \mathcal{V})} \int_{R^{d+3} \times R^{d+3}} |\zeta - \xi|^q d\pi(\zeta, \xi) \right\}^{1/q} \quad q \in [1, \infty), \quad (1.8)$$

where  $\Pi(\mathcal{N}, \mathcal{V})$  is the set of probability measures on  $R^{d+3} \times R^{d+3}$  with marginals  $\mathcal{N}$  and  $\mathcal{V}$ . Indeed, this is a natural metric on the set of the Young measures generated by approximate sequences of numerical solutions in view of the available stability estimates. In comparison with the standard Lévy–Prokhorov metric induced by the weak-(\*) topology (on the space of measures), the Wasserstein distance includes a piece of information on large distances in the associated phase space  $R^{d+3}$ .

For scalar conservation laws, the convergence of finite volume methods with respect to the Wasserstein distance has been investigated by Fjordholm and Solem [33]. They proved that monotone finite volume schemes being formally first order schemes show in special situations second order convergence rate in  $W_1$ . On the other hand, the first order rate in  $W_1$  has been proven optimal in general, see [49]. Such a result, however, seems to be out of reach for the Euler system as it would imply strong (a.e. pointwise) convergence of the expected values – the numerical solutions.

The paper is organized as follows. In Section 2 we introduce the concept of consistent approximate solutions. Section 3 summarizes available results on the strong (pointwise) convergence of the approximate solutions and the weak convergence in terms of Young measures. Section 4 is the heart of the paper. We use the theory of  $\mathcal{K}$ -convergence adapted to the Young measures to show that the limiting Young measure can be effectively described by means of the Cesàro averages of the approximate solutions. As an added benefit with respect to available results, we therefore obtain strong convergence of the Cesàro averages in  $L^q((0, T) \times \Omega)$  and the Wasserstein distance  $W_q$  for some  $q \geq 1$ . Finally, in Section 5, we present numerical simulations obtained by two finite volume methods: a recently proposed finite volume method, see [25], that is (entropy)-stable and consistent and thus yields the consistent approximate solutions required by the abstract theory and a more standard finite volume method based on the generalized Riemann problem, see, e.g. [4–7, 13] and the references therein. The predicted strong convergence of the Cesàro averages when approximate solutions experience oscillations is confirmed by both numerical methods. Our numerical results clearly demonstrate robustness of the proposed  $\mathcal{K}$ -convergence technique.

## 2 Approximate solutions

For the sake of simplicity, we focus on the perfect gas with the standard equation of state

$$p = (\gamma - 1)\varrho e, \quad e = \frac{1}{\gamma - 1}\vartheta,$$

where  $e$  is the specific internal energy and  $\vartheta$  the absolute temperature. Accordingly,

$$E = \frac{1}{2} \frac{|\mathbf{m}|^2}{\varrho} + \varrho e, \quad p = (\gamma - 1) \left( E - \frac{1}{2} \frac{|\mathbf{m}|^2}{\varrho} \right).$$

Finally, we introduce the specific entropy

$$s = \log\left(\vartheta^{\frac{1}{\gamma-1}}\right) - \log(\varrho), \text{ and the total entropy } S = \varrho s.$$

**Definition 2.1** (Consistent approximations). We say that  $[\varrho_h, \mathbf{m}_h, E_h]$  is a family of approximate solutions *consistent* with the Euler system (1.1) in  $Q = (0, T) \times \Omega$  if:

- $\varrho_h, \mathbf{m}_h, E_h$  are measurable functions on  $Q$ ,

$$\varrho_h > 0, \quad p_h \equiv (\gamma - 1) \left( E_h - \frac{1}{2} \frac{|\mathbf{m}_h|^2}{\varrho_h} \right) > 0 \text{ a.e. in } Q;$$

- 

$$\left[ \int_{\Omega} \varrho_h \varphi \, dx \right]_{t=0}^{t=\tau} = \int_0^{\tau} \int_{\Omega} [\varrho_h \partial_t \varphi + \mathbf{m}_h \cdot \nabla_x \varphi] \, dx \, dt + \int_0^{\tau} e_{1,h}(t, \varphi) \, dt \quad (2.1)$$

for any  $0 \leq \tau \leq T$ , and any  $\varphi \in C^1([0, T] \times \bar{\Omega})$ , where

$$e_{1,h}(\cdot, \varphi) \rightarrow 0 \text{ in } L^1(0, T) \text{ as } h \searrow 0 \text{ for any fixed } \varphi;$$

- 

$$\left[ \int_{\Omega} \mathbf{m}_h \cdot \varphi \, dx \right]_{t=0}^{t=\tau} = \int_0^{\tau} \int_{\Omega} \left[ \mathbf{m}_h \cdot \partial_t \varphi + \frac{\mathbf{m}_h \otimes \mathbf{m}_h}{\varrho_h} : \nabla_x \varphi + p_h \operatorname{div}_x \varphi \right] \, dx \, dt + \int_0^{\tau} e_{2,h}(t, \varphi) \, dt \quad (2.2)$$

for any  $0 \leq \tau \leq T$ , and any  $\varphi \in C^1([0, T] \times \bar{\Omega}; R^d)$ ,  $\varphi \cdot \mathbf{n}|_{\Omega} = 0$ , where

$$e_{2,h}(\cdot, \varphi) \rightarrow 0 \text{ in } L^1(0, T) \text{ as } h \searrow 0 \text{ for any fixed } \varphi;$$

- 

$$\int_{\Omega} E_h(\tau) \, dx = \int_{\Omega} E_{0,h} \, dx \text{ for any } 0 \leq \tau \leq T. \quad (2.3)$$

In addition, we say that  $[\varrho_h, \mathbf{m}_h, E_h]$  is *admissible* if for the entropy  $s_h$ ,

$$s_h = \log\left(\vartheta_h^{\frac{1}{\gamma-1}}\right) - \log(\varrho_h), \quad \vartheta_h = (\gamma - 1) \frac{1}{\varrho_h} \left( E_h - \frac{1}{2} \frac{|\mathbf{m}_h|^2}{\varrho_h} \right),$$

the entropy inequality holds

$$\left[ \int_{\Omega} \varrho_h \chi(s_h) \varphi \, dx \right]_{t=0}^{t=\tau} \geq \int_0^{\tau} \int_{\Omega} [\varrho_h \chi(s_h) \partial_t \varphi + \chi(s_h) \mathbf{m}_h \cdot \nabla_x \varphi] \, dx \, dt + \int_0^{\tau} e_{3,h}(t, \varphi) \, dt \quad (2.4)$$

for any  $0 \leq \tau \leq T$ , any  $\varphi \in C^1([0, T] \times \bar{\Omega})$ ,  $\varphi \geq 0$ , and any  $\chi$ ,

$$\chi : R \rightarrow R \text{ a non-decreasing concave function, } \chi(s) \leq \bar{\chi} \text{ for all } s \in R,$$

where

$$e_{3,h}(\cdot, \varphi) \rightarrow 0 \text{ in } L^1(0, T) \text{ as } h \searrow 0 \text{ for any fixed } \varphi.$$

A family of approximate solutions provides seemingly less information than the corresponding *weak formulation* of the Euler system (1.1)–(1.3), and (1.4). Nonetheless, as we shall see below, the approximate solutions in the sense of Definition 2.1 generate a measure-valued solution introduced in [10]. In this paper, we focus on the consistent approximate solutions generated by suitable numerical schemes. A specific example of such a scheme – the finite volume method (5.3)–(5.5) – is given in Section 5. However, the concept presented here is quite general allowing to include the vanishing viscosity as well as other types of singular limit perturbations. In particular,  $[\varrho_h, \mathbf{m}_h, E_h]$  may be weak solutions of the Euler system itself (the error terms  $e_{i,h}$ ,  $i = 1, 2, 3$  being zero).

Note that, in contrast with the Euler system (1.1), the approximate solutions satisfy merely the total energy balance (2.3), meaning the last equation in (1.1) is integrated over the physical domain. It can be shown, however, that (2.3), together with the entropy inequality (2.4), give rise to the energy equation as soon as the all quantities are smooth and all error terms set to be zero. The proof is the same as for the Navier–Stokes–Fourier system and we refer the reader to [26] for details.

### 3 Strong vs. weak convergence

We discuss sequential stability of the set of approximate solutions introduced in Definition 2.1. To this end, we suppose that the corresponding initial data satisfy

$$\begin{aligned} \varrho_h(0, \cdot) = \varrho_{0,h}, \quad \mathbf{m}_h(0, \cdot) = \mathbf{m}_{0,h}, \quad E_h(0, h) = E_{0,h}, \quad \varrho_{0,h} > 0, \quad E_{0,h} - \frac{1}{2} \frac{|\mathbf{m}_{0,h}|^2}{\varrho_{0,h}} > 0, \\ \int_{\Omega} E_{0,h} \, dx \leq \mathcal{E}_0 \text{ uniformly for } h \searrow 0; \end{aligned} \quad (3.1)$$

and

$$\begin{aligned} s_h(0, \cdot) \equiv \log(\vartheta_{0,h}^{\frac{1}{\gamma-1}}) - \log(\varrho_{0,h}) \geq \underline{s} > -\infty \text{ uniformly for } h \searrow 0, \\ \text{where } \vartheta_{0,h} \equiv (\gamma - 1) \frac{1}{\varrho_{0,h}} \left( E_{0,h} - \frac{1}{2} \frac{|\mathbf{m}_{0,h}|^2}{\varrho_{0,h}} \right). \end{aligned} \quad (3.2)$$

The uniform bound (3.1) imposed on the initial energy, together with the total energy balance (2.3), yield

$$\int_{\Omega} E_h(\tau, \cdot) \, dx \leq \mathcal{E}_0 \text{ uniformly for } h \searrow 0, \quad 0 \leq \tau \leq T, \quad (3.3)$$

in particular,

$$\int_{\Omega} \frac{1}{2} \frac{|\mathbf{m}_h|^2}{\varrho_h}(\tau, \cdot) \, dx \leq \mathcal{E}_0. \quad (3.4)$$

Next, we *suppose*, in accordance with the fact that the entropy is transported along streamlines, that

$$s_h(\tau, \cdot) \geq \underline{s} \text{ for all } 0 \leq \tau \leq T. \quad (3.5)$$

**Remark 3.1.** Note that (3.5) actually follows from (3.2) as soon as the error term in (2.4) vanishes or, alternatively,

$$e_{3,h}(t, \psi) \equiv 0 \text{ for any } \psi = \psi(t),$$

see [25, Section 4.2] for details.

Anticipating (3.5) we may rewrite the total energy in terms of  $\varrho_h, \mathbf{m}_h, s_h$  as

$$E_h = \frac{1}{2} \frac{|\mathbf{m}_h|^2}{\varrho_h} + \frac{1}{\gamma - 1} \varrho_h^\gamma \exp [(\gamma - 1)s_h].$$

In view of (3.3)–(3.5) we obtain

$$\int_{\Omega} \varrho_h^\gamma(\tau, \cdot) \, dx \lesssim \mathcal{E}_0 \text{ uniformly in } \tau, h, \quad (3.6)$$

and

$$\int_{\Omega} \mathbf{m}_h^{\frac{2\gamma}{\gamma+1}}(\tau, \cdot) \, dx \lesssim \mathcal{E}_0 \text{ uniformly in } \tau, h. \quad (3.7)$$

Finally, introducing the total entropy  $S_h \equiv \varrho_h(s_h - \underline{s}) \geq 0$ , we deduce

$$\int_{\Omega} S_h^\gamma(\tau, \cdot) \, dx \lesssim \mathcal{E}_0 \text{ uniformly in } \tau, h, \quad (3.8)$$

and

$$\int_{\Omega} \left( \frac{S_h^2}{\varrho_h} \right)^\gamma(\tau, \cdot) \, dx \lesssim \mathcal{E}_0 \text{ uniformly in } \tau, h, \quad (3.9)$$

see [8, Section 3.2] for details.

### 3.1 Strong (pointwise) convergence

Note that all the uniform estimates established so far yield only boundedness of the approximate solutions in various  $L^p$ -spaces. The appropriate notion of convergence is therefore “weak”, or, more precisely, “weak- $(*)$ ” convergence, meaning convergence in the sense of integral averages. As already pointed out, this is of little practical importance as the limits of oscillating quantities are difficult to identify.

However, the convergence is strong (pointwise a.e.) as soon as the limit Euler system (1.1)–(1.3) admits a (unique) strong solution. Indeed any *admissible* sequence of consistent approximate solutions  $[\varrho_h, \mathbf{m}_h, E_h]$  generates a dissipative measure-valued (DMV) solution in the sense of [10]. The (DMV) solutions enjoy the weak-strong uniqueness property yielding the desired conclusion. The relevant result can be stated as follows, cf. [10, Theorem 3.3]:



**Proposition 3.2.** *Let  $\Omega \subset R^d$ ,  $d = 1, 2, 3$  be a bounded Lipschitz domains. Let  $\{\varrho_h, \mathbf{m}_h, E_h\}_{h \searrow 0}$  be a family of admissible approximate solutions consistent with the Euler system in the sense of Definition 2.1. Let the approximate initial data satisfy (3.1), (3.2), and suppose that (3.5) holds. Let*

$$\varrho_{0,h} \rightarrow \varrho_0 > 0, \quad \mathbf{m}_{0,h} \rightarrow \mathbf{m}_0, \quad E_{0,h} \rightarrow E_0 > 0,$$

$$s_h(0, \cdot) \equiv \frac{1}{\gamma - 1} \log \left( \frac{\gamma - 1}{\varrho_{0,h}} \left( E_{0,h} - \frac{1}{2} \frac{|\mathbf{m}_{0,h}|^2}{\varrho_{0,h}} \right) \right) - \log(\varrho_{0,h}) \rightarrow s_0 \text{ weakly in } L^1(\Omega) \text{ as } h \searrow 0,$$

where

$$s_0 = \frac{1}{\gamma - 1} \log \left( \frac{\gamma - 1}{\varrho_0} \left( E_0 - \frac{1}{2} \frac{|\mathbf{m}_0|^2}{\varrho_0} \right) \right) - \log(\varrho_0).$$

Finally, suppose that the Euler system (1.1), (1.2), with the initial data (1.3), admits a strong solution  $[\varrho, \mathbf{m}, E]$  Lipschitz continuous in  $[0, T] \times \bar{\Omega}$ .

Then

$$\varrho_h \rightarrow \varrho, \quad \mathbf{m}_h \rightarrow \mathbf{m}, \quad E_h \rightarrow E \text{ in } L^1((0, T) \times \Omega) \text{ as } h \searrow 0.$$

Note that the convergence stated in Proposition 3.2 is unconditional, meaning it is not necessary to consider subsequences, as the limit solution is unique.

### 3.2 Weak convergence

If the limit system fails to possess a classical solution, the convergence might not be strong. In such a case, the nonlinear composition operators do not commute with weak limits and the limit object may not be even a weak solution of the Euler system.

To analyze the weak convergence, it is convenient to work with the variables  $[\varrho_h, \mathbf{m}_h, S_h]$ . In view of the uniform bounds (3.6)–(3.8) we obtain that

$$\begin{aligned} \varrho_h &\rightarrow \varrho \text{ weakly-}^* \text{ in } L^\infty(0, T; L^\gamma(\Omega)), \\ \mathbf{m}_h &\rightarrow \mathbf{m} \text{ weakly-}^* \text{ in } L^\infty(0, T; L^{\frac{2\gamma}{\gamma+1}}(\Omega; R^d)), \\ S_h &\rightarrow S \text{ weakly-}^* \text{ in } L^\infty(0, T; L^\gamma(\Omega)) \end{aligned} \tag{3.10}$$

passing to suitable subsequences as the case may be. The key quantity is the total energy

$$E_h = \frac{1}{2} \frac{|\mathbf{m}_h|^2}{\varrho_h} + \frac{a}{\gamma - 1} \varrho_h^\gamma \exp \left( (\gamma - 1) \frac{S_h}{\varrho_h} \right),$$

where  $a = \exp((\gamma - 1)\underline{s})$ . Note that

$$[\varrho, \mathbf{m}, S] \mapsto E(\varrho, \mathbf{m}, S) \equiv \begin{cases} \frac{1}{2} \frac{|\mathbf{m}|^2}{\varrho} + \frac{a}{\gamma - 1} \varrho^\gamma \exp \left( (\gamma - 1) \frac{S}{\varrho} \right), & \text{if } \varrho > 0 \\ 0, & \text{if } \varrho = |\mathbf{m}| = 0 \text{ and } S \leq 0 \\ \infty, & \text{otherwise} \end{cases}$$

is a convex lower semicontinuous function on  $R^{d+2}$ , smooth and strictly convex for  $\varrho > 0$  and  $S$ , see [8, Lemma 3.1]. Considering a subsequence if necessary, we conclude that

$$\{\varrho_h, \mathbf{m}_h, S_h, E_h\}_{h>0} \text{ generates a Young measure } \mathcal{V}_{t,x} \in \mathcal{P}(R^{d+3}), (t, x) \in Q.$$

In addition we introduce a *marginal*  $\nu_{t,x} \in \mathcal{P}(R^{d+2})$ , such that

$$\langle \nu_{t,x}, g(\tilde{\varrho}_h, \tilde{\mathbf{m}}_h, \tilde{S}_h) \rangle \equiv \langle \mathcal{V}_{t,x}, g(\tilde{\varrho}_h, \tilde{\mathbf{m}}_h, \tilde{S}_h) 1_R(\tilde{E}) \rangle \text{ for all } g \in BC(R^{d+2}).$$

Moreover, we have

$$\begin{aligned} E_h &\rightarrow E \text{ weakly-}^* \text{ in } L^\infty(0, T; \mathcal{M}^+(\bar{\Omega})), \\ \frac{1}{2} \frac{|\mathbf{m}|^2}{\varrho} + \frac{a}{\gamma-1} \varrho^\gamma \exp\left((\gamma-1) \frac{S}{\varrho}\right) &\leq \left\langle \nu; \frac{1}{2} \frac{|\tilde{\mathbf{m}}|^2}{\tilde{\varrho}} + \frac{a}{\gamma-1} \tilde{\varrho}^\gamma \exp\left((\gamma-1) \frac{\tilde{S}}{\tilde{\varrho}}\right) \right\rangle \leq E, \end{aligned}$$

where the first inequality is Jensen's inequality, while the second follows from the arguments of [23, Lemma 2.1] applied to  $F = 0$ ,  $G = E$  and  $Z = (\tilde{\varrho}, \tilde{\mathbf{m}}, \tilde{S})$ . Using the energy conservation (2.3) we obtain

$$\int_{\bar{\Omega}} E(\tau) = \lim_{h \rightarrow 0} \int_{\Omega} \left[ \frac{1}{2} \frac{|\mathbf{m}_{0,h}|^2}{\varrho_{0,h}} + \frac{a}{\gamma-1} \varrho_{0,h}^\gamma \exp\left((\gamma-1) \frac{S_{0,h}}{\varrho_{0,h}}\right) \right] dx \text{ for a.a. } \tau \in [0, T].$$

We proceed by introducing the oscillation defect

$$\begin{aligned} \mathbf{osc}[\varrho_h, \mathbf{m}_h, S_h] &\equiv \left\langle \nu; \frac{1}{2} \frac{|\tilde{\mathbf{m}}|^2}{\tilde{\varrho}} + \frac{a}{\gamma-1} \tilde{\varrho}^\gamma \exp\left((\gamma-1) \frac{\tilde{S}}{\tilde{\varrho}}\right) \right\rangle - \left[ \frac{1}{2} \frac{|\mathbf{m}|^2}{\varrho} + \frac{a}{\gamma-1} \varrho^\gamma \exp\left((\gamma-1) \frac{S}{\varrho}\right) \right] \geq 0; \end{aligned}$$

the concentration defect

$$\mathbf{conc}[\varrho_h, \mathbf{m}_h, S_h] \equiv E - \left\langle \nu; \frac{1}{2} \frac{|\tilde{\mathbf{m}}|^2}{\tilde{\varrho}} + \frac{a}{\gamma-1} \tilde{\varrho}^\gamma \exp\left((\gamma-1) \frac{\tilde{S}}{\tilde{\varrho}}\right) \right\rangle \geq 0;$$

and the total energy defect

$$\mathbf{edef}[\varrho_h, \mathbf{m}_h, S_h] = \mathbf{osc}[\varrho_h, \mathbf{m}_h, S_h] + \mathbf{conc}[\varrho_h, \mathbf{m}_h, S_h] = E - \left[ \frac{1}{2} \frac{|\mathbf{m}|^2}{\varrho} + \frac{a}{\gamma-1} \varrho^\gamma \exp\left((\gamma-1) \frac{S}{\varrho}\right) \right].$$

Note that  $\mathbf{osc}[\varrho_h, \mathbf{m}_h, S_h] \in L^\infty(0, T; L^1(\Omega))$ , while

$$\mathbf{conc}[\varrho_h, \mathbf{m}_h, S_h], \mathbf{edef}[\varrho_h, \mathbf{m}_h, S_h] \in L^\infty(0, T; \mathcal{M}^+(\bar{\Omega})).$$

The following observations are standard:

$$\begin{aligned} \mathbf{osc}[\varrho_h, \mathbf{m}_h, S_h]|_B = 0 &\Leftrightarrow \varrho_h \rightarrow \varrho, \mathbf{m}_h \rightarrow \mathbf{m}, S_h \rightarrow S \text{ a.e. in } B \text{ (up to a subsequence);} \\ \mathbf{conc}[\varrho_h, \mathbf{m}_h, S_h]|_{\overline{B}} = 0 &\Leftrightarrow E_h \rightarrow E \text{ weakly in } L^1(B); \\ \mathbf{edef}[\varrho_h, \mathbf{m}_h, S_h]|_{\overline{B}} = 0 &\Leftrightarrow \varrho_h \rightarrow \varrho, \mathbf{m}_h \rightarrow \mathbf{m}, S_h \rightarrow S, E_h \equiv E(\varrho_h, \mathbf{m}_h, S_h) \rightarrow E \text{ in } L^1(B) \end{aligned}$$

for any Borel set  $B \subset [0, T] \times \overline{\Omega}$ .

Finally, we report the following result, see Chaudhuri [12], which can be obtained in analogously way as in [24] due to the convexity of pressure.

**Proposition 3.3.** *Let  $\Omega \subset R^d$ ,  $d = 1, 2, 3$  be a bounded Lipschitz domain. Let  $\{\varrho_h, \mathbf{m}_h, E_h\}_{h \searrow 0}$  be a family of admissible approximate solutions consistent with the Euler system in the sense of Definition 2.1 such that*

$$\begin{aligned} \varrho_h &\rightarrow \varrho \text{ weakly-}^* \text{ in } L^\infty(0, T; L^\gamma(\Omega)), \\ \mathbf{m}_h &\rightarrow \mathbf{m} \text{ weakly-}^* \text{ in } L^\infty(0, T; L^{\frac{2\gamma}{\gamma+1}}(\Omega; R^d)), \\ S_h &\rightarrow S \text{ weakly-}^* \text{ in } L^\infty(0, T; L^\gamma(\Omega)), \end{aligned}$$

and

$$E_h \equiv \frac{1}{2} \frac{|\mathbf{m}_h|^2}{\varrho_h} + \frac{a}{\gamma-1} \varrho_h^\gamma \exp\left((\gamma-1) \frac{S_h}{\varrho_h}\right) \rightarrow E \text{ in } L^\infty(0, T; \mathcal{M}^+(\overline{\Omega})).$$

Suppose that there is an open neighborhood  $U$  of  $\partial\Omega$  such that

$$\mathbf{edef}[\varrho_h, \mathbf{m}_h, S_h]|_{[0, T] \times \overline{U}} = 0.$$

Finally, suppose that the limit  $[\varrho, \mathbf{m}, S]$  is a weak solution of the Euler system in  $\mathcal{D}'((0, T) \times \Omega)$ , in particular,

$$\partial_t \mathbf{m} + \operatorname{div}_x \left( \frac{\mathbf{m} \otimes \mathbf{m}}{\varrho} \right) + \nabla_x p(\varrho, S) = 0 \text{ in } \mathcal{D}'((0, T) \times \Omega).$$

Then

$$\mathbf{edef}[\varrho_h, \mathbf{m}_h, S_h] \equiv 0,$$

and

$$\varrho_h \rightarrow \varrho, \mathbf{m}_h \rightarrow \mathbf{m}, S_h \rightarrow S, E_h \rightarrow E \text{ in } L^1((0, T) \times \Omega).$$

Proposition 3.3 asserts that as long as the convergence of approximate solutions is strong in a neighborhood of the boundary and the limit is a weak solution of the Euler system, then the convergence must be strong everywhere. A very rough extrapolation might be that either the convergence is strong or the limit object *is not* a weak solution of the limit system. Such a result might be seen as a sharp version of the celebrated Lax-Wendroff theorem [41] which states that a bounded sequence of pointwisely convergent numerical solutions, that are generated by a consistent, conservative and entropy stable numerical scheme, converges to a weak entropy solution.

## 4 $\mathcal{K}$ -convergence of Young measures

Accepting the conclusion of Proposition 3.3 as an evidence that oscillating (weakly converging) sequences of approximate solutions may give rise to “truly” measure-valued solutions, we might want to compute the distribution of the associated Young measure. Unfortunately, the method proposed in [30, 31] asserts only the weak-(\*) convergence of these objects featuring the same difficulties to be captured numerically as oscillating solutions. Here, we propose *a new method* based on the concept of  $\mathcal{K}$ -convergence developed in the context of Young measures by Balder [1, 2].

Evoking the situation described in Section 3, we consider a Young measure  $\mathcal{V}_{t,x}$  generated by a sequence of admissible approximate solutions  $[\varrho_h, \mathbf{m}_h, S_h, E_h]$  consistent with the Euler system. Note that we have deliberately included the conservative variables in order to capture correctly shock positions and to provide a direct comparison with the results [30, 31]. The Young measure adapted variant of the celebrated Prokhorov theorem proved by Balder [2], [1, Theorem 3.15] asserts the existence of a suitable subsequence such that

$$\frac{1}{N} \sum_{n=1}^N \delta_{[\varrho_{h_n}(t,x), \mathbf{m}_{h_n}(t,x), S_{h_n}(t,x), E_{h_n}(t,x)]} \rightarrow \mathcal{V}_{t,x} \text{ as } N \rightarrow \infty \text{ narrowly in } \mathcal{P}(R^{d+3}) \quad (4.1)$$

for a.a.  $(t, x) \in Q$ .

Here and hereafter, the symbol  $\delta_Y$  denotes the Dirac mass supported at the point  $Y$ . Moreover, in view of Castaign, de Fitte, and Valadier [11, Lemma 6.5.17] and the Komlós theorem [39], the above sequence can be chosen in such a way that the barycenters converge:

$$\begin{aligned} \frac{1}{N} \sum_{n=1}^N \varrho_{h_n}(t, x) &\rightarrow \varrho(t, x) \equiv \langle \mathcal{V}_{t,x}; \tilde{\varrho} \rangle, \\ \frac{1}{N} \sum_{n=1}^N \mathbf{m}_{h_n}(t, x) &\rightarrow \mathbf{m}(t, x) \equiv \langle \mathcal{V}_{t,x}; \tilde{\mathbf{m}} \rangle, \\ \frac{1}{N} \sum_{n=1}^N S_{h_n}(t, x) &\rightarrow S(t, x) \equiv \langle \mathcal{V}_{t,x}; \tilde{S} \rangle, \\ \frac{1}{N} \sum_{n=1}^N E_{h_n}(t, x) &\rightarrow \bar{E}(t, x) \equiv \langle \mathcal{V}_{t,x}; \tilde{E} \rangle \end{aligned} \quad (4.2)$$

for a.a.  $(t, x) \in Q$ . Finally, in view of (3.10) and the standard Banach–Sacks theorem, the conver-

gence of the density, momentum and entropy can be strengthened to

$$\begin{aligned} \frac{1}{N} \sum_{n=1}^N \varrho_{h_n} &\rightarrow \varrho \text{ in } L^\gamma((0, T) \times \Omega) \\ \frac{1}{N} \sum_{n=1}^N \mathbf{m}_{h_n} &\rightarrow \mathbf{m} \text{ in } L^{\frac{2\gamma}{\gamma+1}}((0, T) \times \Omega; R^d) \\ \frac{1}{N} \sum_{n=1}^N S_{h_n} &\rightarrow S \text{ in } L^\gamma((0, T) \times \Omega). \end{aligned} \quad (4.3)$$

As observed in Section 3, we have  $\bar{E} \leq E$ , where  $E$  is the weak- $(*)$  limit of  $E_{h_n}$  in  $L^\infty(0, T; \mathcal{M}^+(\bar{\Omega}))$ . Moreover, from the Fatou-Vitali theorem for the Young measures [1, Theorem 3.13] we also deduce

$$\int_0^T \int_\Omega \langle \nu_{t,x}, E(\tilde{\varrho}, \tilde{\mathbf{m}}, \tilde{S})(t, x) \rangle dx dt \leq \liminf_{N \rightarrow \infty} \int_0^T \int_\Omega \frac{1}{N} \sum_{n=1}^N E_{h_n}(t, x) dx dt. \quad (4.4)$$

As a consequence of (4.2)–(4.4), we can extend (4.1) as follows:

**Lemma 4.1.** *Let*

$$\bar{\mathcal{V}}_{t,x}^N \equiv \frac{1}{N} \sum_{n=1}^N \delta_{[\varrho_{h_n}, \mathbf{m}_{h_n}, S_{h_n}, E_{h_n}](t,x)} \in \mathcal{P}(R^{d+3})$$

be the family of Cesàro averages of the Young measures in (4.1).

Then

$$\langle \bar{\mathcal{V}}_{t,x}^N, g(\tilde{\varrho}, \tilde{\mathbf{m}}, \tilde{S}) \rangle \rightarrow \langle \mathcal{V}_{t,x}, g(\tilde{\varrho}, \tilde{\mathbf{m}}, \tilde{S}) \rangle \text{ as } N \rightarrow \infty \text{ for a.a. } (t, x) \in Q \quad (4.5)$$

for any function  $g \in C(R^{d+2})$ ,

$$|g(z)| \leq 1 + |z|^q, \quad 1 \leq q < \frac{2\gamma}{\gamma+1}.$$

*Proof.* Decomposing  $g$  into positive and negative part,  $g = g^+ + g^-$  we may assume, without loss of generality, that  $g \geq 0$ . Let  $T_K$  be a family of cut-off functions,

$$T_K(z) = \min(z, K), \quad K \geq 0.$$

We write

$$\langle \bar{\mathcal{V}}_{t,x}^N, g(\tilde{\varrho}, \tilde{\mathbf{m}}, \tilde{S}) \rangle = \left\langle \bar{\mathcal{V}}_{t,x}^N, T_K \left( g(\tilde{\varrho}, \tilde{\mathbf{m}}, \tilde{S}) \right) \right\rangle + \left\langle \bar{\mathcal{V}}_{t,x}^N, (Id - T_K) \left( g(\tilde{\varrho}, \tilde{\mathbf{m}}, \tilde{S}) \right) \right\rangle.$$

In virtue of (4.1) we have

$$\left\langle \bar{\mathcal{V}}_{t,x}^N, T_K \left( g(\tilde{\varrho}, \tilde{\mathbf{m}}, \tilde{S}) \right) \right\rangle \rightarrow \left\langle \mathcal{V}_{t,x}, T_K \left( g(\tilde{\varrho}, \tilde{\mathbf{m}}, \tilde{S}) \right) \right\rangle \text{ for a.a. } (t, x) \in Q.$$

On the other hand,

$$\begin{aligned} \left| \left\langle \bar{\mathcal{V}}_{t,x}^N, (Id - T_K) \left( g(\tilde{\varrho}, \tilde{\mathbf{m}}, \tilde{S}) \right) \right\rangle \right| &\leq \left\langle \bar{\mathcal{V}}_{t,x}^N, \chi_{g(\tilde{\varrho}, \tilde{\mathbf{m}}, \tilde{S}) \geq K} g(\tilde{\varrho}, \tilde{\mathbf{m}}, \tilde{S}) \right\rangle \leq \\ &\left\langle \bar{\mathcal{V}}_{t,x}^N, \chi_{g(\tilde{\varrho}, \tilde{\mathbf{m}}, \tilde{S}) \geq K} \frac{1}{g(\tilde{\varrho}, \tilde{\mathbf{m}}, \tilde{S})^\alpha} g(\tilde{\varrho}, \tilde{\mathbf{m}}, \tilde{S})^{1+\alpha} \right\rangle \leq \frac{1}{K^\alpha} \left\langle \bar{\mathcal{V}}_{t,x}^N, g(\tilde{\varrho}, \tilde{\mathbf{m}}, \tilde{S})^{1+\alpha} \right\rangle. \end{aligned}$$

Seeing that

$$\tilde{\varrho}^\gamma + \tilde{S}^\gamma + |\tilde{\mathbf{m}}|^{\frac{2\gamma}{\gamma+1}} \lesssim \frac{1}{2} \frac{|\tilde{\mathbf{m}}|^2}{\tilde{\varrho}} + \frac{1}{\gamma-1} \tilde{\varrho}^\gamma \exp\left(\left(\gamma-1\right)\frac{\tilde{S}}{\tilde{\varrho}}\right)$$

we may infer there exists  $\alpha > 0$  small enough so that

$$\left\langle \bar{\mathcal{V}}_{t,x}^N, g(\tilde{\varrho}, \tilde{\mathbf{m}}, \tilde{S})^{1+\alpha} \right\rangle \lesssim \left\langle \bar{\mathcal{V}}_{t,x}^N, E(\tilde{\varrho}, \tilde{\mathbf{m}}, \tilde{S}) \right\rangle = \frac{1}{N} \sum_{n=1}^N E_{h_n}(t, x) \text{ for a.a. } (t, x) \in Q.$$

Consequently using the convergence stated in (4.2) and the Levy monotone convergence theorem we may pass to the limit  $K \rightarrow \infty$  obtaining the desired conclusion.  $\square$

## 4.1 Strong convergence in the Wasserstein distance

Relation (4.1) asserts narrow convergence of the Cesàro averages  $\bar{\mathcal{V}}^N$  to the Young measure  $\mathcal{V}$  that is (a.e.) pointwise with respect to the parameter  $(t, x)$  in the physical space  $Q$ . It is legitimate to ask whether this can be strengthened to the convergence in the Wasserstein metric. We first observe that

$$W_1\left(\bar{\mathcal{V}}_{t,x}^N, \mathcal{V}_{t,x}\right) \rightarrow 0 \text{ as } N \rightarrow \infty \text{ for a.a. } (t, x) \in Q. \quad (4.6)$$

Indeed, as the narrow convergence has been established in (4.1), relation (4.6) follows as soon as we observe the convergence of first moments for a.a.  $(t, x) \in Q$ , see Villani [52, Definition 6.8, Theorem 6.9]:

$$\left\langle \bar{\mathcal{V}}_{t,x}^N, |\tilde{\varrho}| + |\tilde{\mathbf{m}}| + |\tilde{S}| + |\tilde{E}| \right\rangle \equiv \frac{1}{N} \sum_{h_n=1}^N (\varrho_{h_n} + |\mathbf{m}_{h_n}| + S_{h_n} + E_{h_n}) \rightarrow \langle \mathcal{V}_{t,x}, \tilde{\varrho} + |\tilde{\mathbf{m}}| + \tilde{S} + \tilde{E} \rangle. \quad (4.7)$$

However, relation (4.7) follows directly from Lemma 4.1 and the last statement in (4.2).

Our next goal is to investigate the convergence of the Cesàro sums of the marginals,

$$\bar{\nu}_{t,x}^N \equiv \frac{1}{N} \sum_{n=1}^N \nu_{h_n} \equiv \frac{1}{N} \sum_{n=1}^N \delta_{[\varrho_{h_n}, \mathbf{m}_{h_n}, S_{h_n}]}(t, x) \in \mathcal{P}(R^{d+2}).$$

Specifically, we show that

$$\|W_q(\bar{\nu}^N, \nu)\|_{L^q(Q)} \rightarrow 0 \text{ as } N \rightarrow \infty \text{ for some } q \geq 1. \quad (4.8)$$

Using the definition of the Wasserstein distance we have the following inequality

$$|W_q(\bar{\nu}_{t,x}^N, \nu_{t,x})| \leq \langle \bar{\nu}_{t,x}^N, |\tilde{\varrho}|^q + |\tilde{\mathbf{m}}|^q + |\tilde{S}|^q \rangle + \langle \nu_{t,x}, |\tilde{\varrho}|^q + |\tilde{\mathbf{m}}|^q + |\tilde{S}|^q \rangle. \quad (4.9)$$

Now, the two terms on the right-hand side are bounded in  $L^q(Q)$ ,  $1 \leq q \leq \frac{2\gamma}{\gamma+1}$  due to the convergences established in (4.2) and (4.4). Combining this with (4.6) we conclude that

$$\|W_q(\bar{\nu}^N, \nu)\|_{L^q(Q)} \rightarrow 0 \quad \text{as } N \rightarrow \infty \text{ for any } 1 \leq q < \frac{2\gamma}{\gamma+1}. \quad (4.10)$$

Summing up the previous discussion, we can state the main result of the present paper.

**Theorem 4.2.** *Let  $\Omega \subset R^d$ ,  $d = 1, 2, 3$  be a bounded Lipschitz domain. Let  $\{\varrho_h, \mathbf{m}_h, S_h, E_h\}_{h \searrow 0}$  be a family of admissible approximate solutions consistent with the Euler system in the sense of Definition 2.1. Let the approximate initial data satisfy (3.1), (3.2), and let (3.5) hold.*

*Then there exists a subsequence  $h_n \rightarrow 0$  such that the following hold:*

- *the sequence  $\{\varrho_{h_n}, \mathbf{m}_{h_n}, S_{h_n}, E_{h_n}\}_{n=1}^\infty$  generates a Young measure  $\{\mathcal{V}_{t,x}\}_{(t,x) \in Q} \in \mathcal{P}(R^{d+3})$ , with a marginal  $\{\nu_{t,x}\}_{(t,x) \in Q} \in \mathcal{P}(R^{d+2})$ ,*

$$\left\langle \nu_{t,x}; g(\tilde{\varrho}, \tilde{\mathbf{m}}, \tilde{S}) \right\rangle \equiv \left\langle \mathcal{V}_{t,x}; g(\tilde{\varrho}, \tilde{\mathbf{m}}, \tilde{S}) 1_R(\tilde{E}) \right\rangle, \quad g \in BC(R^{d+2});$$

- 

$$W_1(\bar{\mathcal{V}}_{t,x}^N, \mathcal{V}_{t,x}) \rightarrow 0 \text{ as } N \rightarrow \infty \text{ for a.a. } (t,x) \in Q,$$

*for the Cesàro averages*

$$\bar{\mathcal{V}}_{t,x}^N \equiv \frac{1}{N} \sum_{n=1}^N \delta_{[\varrho_{h_n}, \mathbf{m}_{h_n}, S_{h_n}, E_{h_n}]}(t,x) \in \mathcal{P}(R^{d+3});$$

- 

$$\|W_q(\bar{\nu}_{t,x}^N, \nu_{t,x})\|_{L^q(Q)} \rightarrow 0 \text{ as } N \rightarrow \infty \text{ for any } 1 \leq q < \frac{2\gamma}{\gamma+1}$$

*for the Cesàro averages*

$$\bar{\nu}_{t,x}^N \equiv \frac{1}{N} \sum_{n=1}^N \delta_{[\varrho_{h_n}, \mathbf{m}_{h_n}, S_{h_n}]}(t,x) \in \mathcal{P}(R^{d+2}).$$

## 4.2 Convergence in first variation

Using (4.3) we may show convergence of the first variation of the measures  $\bar{\nu}_{t,x}^N$ . Indeed,

$$\begin{aligned} \langle \bar{\nu}_{t,x}^N; |\tilde{\varrho} - \langle \bar{\nu}_{t,x}^N; \tilde{\varrho} \rangle| \rangle &= \frac{1}{N} \sum_{n=1}^N \left| \varrho_{h_n}(t, x) - \left( \frac{1}{N} \sum_{n=1}^N \varrho_{h_n}(t, x) \right) \right| \\ &= \frac{1}{N} \sum_{n=1}^N \left| \varrho_{h_n}(t, x) - \varrho(t, x) + \varrho(t, x) - \left( \frac{1}{N} \sum_{n=1}^N \varrho_{h_n}(t, x) \right) \right|, \end{aligned}$$

where, by virtue of (4.2),

$$\varrho(t, x) - \left( \frac{1}{N} \sum_{n=1}^N \varrho_{h_n}(t, x) \right) \rightarrow 0 \text{ as } N \rightarrow \infty.$$

Next,

$$\frac{1}{N} \sum_{n=1}^N |\varrho_{h_n}(t, x) - \varrho(t, x)| = \langle \bar{\nu}_{t,x}^N; \chi_R (|\tilde{\varrho} - \varrho(t, x)|) \rangle + \langle \bar{\nu}_{t,x}^N; (1 - \chi_R) (|\tilde{\varrho} - \varrho(t, x)|) \rangle,$$

where  $\chi_R$  is a bounded cut-off function. In accordance with (4.1), we have

$$\langle \bar{\nu}_{t,x}^N; \chi_R (|\tilde{\varrho} - \varrho(t, x)|) \rangle \rightarrow \langle \nu_{t,x}; \chi_R (|\tilde{\varrho} - \varrho(t, x)|) \rangle \text{ for a.a. } (t, x) \in Q \text{ and any fixed } R,$$

while, by virtue of (3.1),

$$\int_0^T \int_{\Omega} |\langle \bar{\nu}_{t,x}^N; (1 - \chi_R) (|\tilde{\varrho} - \varrho(t, x)|) \rangle| \, dx \, dt \rightarrow 0 \text{ as } R \rightarrow \infty \text{ uniformly in } N.$$

As, finally,

$$\langle \nu_{t,x}; \chi_R (|\tilde{\varrho} - \varrho(t, x)|) \rangle \rightarrow \langle \nu_{t,x}; (|\tilde{\varrho} - \langle \nu_{t,x}; \tilde{\varrho} \rangle|) \rangle \text{ as } R \rightarrow \infty \text{ for a.a. } (t, x) \in Q,$$

we may infer that

$$\left\| \langle \bar{\nu}_{t,x}^N; |\tilde{\varrho} - \langle \bar{\nu}_{t,x}^N; \tilde{\varrho} \rangle| \rangle - \langle \nu_{t,x}; |\tilde{\varrho} - \langle \nu_{t,x}; \tilde{\varrho} \rangle| \rangle \right\|_{L^1(Q)} \rightarrow 0 \text{ as } N \rightarrow \infty. \quad (4.11)$$

Analogously, we have

$$\left\| \langle \bar{\nu}_{t,x}^N; |\tilde{\mathbf{m}} - \langle \bar{\nu}_{t,x}^N; \tilde{\mathbf{m}} \rangle| \rangle - \langle \nu_{t,x}; |\tilde{\mathbf{m}} - \langle \nu_{t,x}; \tilde{\mathbf{m}} \rangle| \rangle \right\|_{L^1(Q)} \rightarrow 0 \text{ as } N \rightarrow \infty \quad (4.12)$$

and

$$\left\| \langle \bar{\nu}_{t,x}^N; |\tilde{S} - \langle \bar{\nu}_{t,x}^N; \tilde{S} \rangle| \rangle - \langle \nu_{t,x}; |\tilde{S} - \langle \nu_{t,x}; \tilde{S} \rangle| \rangle \right\|_{L^1(Q)} \rightarrow 0 \text{ as } N \rightarrow \infty. \quad (4.13)$$



Unlike  $\varrho_h$ ,  $\mathbf{m}_h$ ,  $S_h$  the energy  $E_h$  is not equi-integrable therefore its momentum cannot be estimated as in (4.11), (4.12). Although it may be seen that (4.11)–(4.12) follow directly from the convergence in the Wasserstein distance as shown in Section 4.1, the convergence of the variance

$$\begin{aligned} & \left\langle \bar{\nu}_{t,x}^N; \left| \tilde{\varrho} - \langle \bar{\nu}_{t,x}^N; \tilde{\varrho} \rangle \right| \right\rangle + \left\langle \bar{\nu}_{t,x}^N; \left| \tilde{\mathbf{m}} - \langle \bar{\nu}_{t,x}^N; \tilde{\mathbf{m}} \rangle \right| \right\rangle + \left\langle \bar{\nu}_{t,x}^N; \left| \tilde{S} - \langle \bar{\nu}_{t,x}^N; \tilde{S} \rangle \right| \right\rangle = \\ & \frac{1}{N} \sum_{n=1}^N \left| \varrho_{h_n} - \frac{1}{N} \sum_{j=1}^N \varrho_{h_j} \right| + \frac{1}{N} \sum_{n=1}^N \left| \mathbf{m}_{h_n} - \frac{1}{N} \sum_{j=1}^N \mathbf{m}_{h_j} \right| + \frac{1}{N} \sum_{n=1}^N \left| S_{h_n} - \frac{1}{N} \sum_{j=1}^N S_{h_j} \right| \end{aligned} \quad (4.14)$$

is directly computable performing simulations on  $N$  different grids with the size  $h_n$ ,  $n = 1, \dots, N$ .

## 5 Finite volume methods

In this section we demonstrate robustness of the new concept of  $\mathcal{K}$ -convergence and apply it to two different finite volume schemes. We consider first a finite volume method that has been derived in our recent paper [25], based on the work of Brenner [9] and Guermond and Popov [35]. In what follows we will refer to it as the *FLM finite volume method*. The latter is an example of a consistent entropy stable finite volume numerical scheme whose solutions  $[\varrho_h, \mathbf{m}_h, E_h]$  satisfy (2.1)–(2.4) and thus serves as an example to illustrate the abstract theory and rigorous convergence proofs.

The second finite volume method is a well-known second order finite volume method based on the generalized Riemann problem, see, e.g., [4, 5, 7, 44, 45]. In what follows we will refer to it as the *GRP finite volume method*. Its theoretical convergence analysis may be an interesting question for future study. We will consider the classical benchmark problems, the Kelvin-Helmholtz and Richtmyer-Meshkov tests. Due to the oscillatory solution behaviour the standard mesh convergence study will indicate that neither of the finite volume methods converges. However, we will demonstrate the strong convergence of the Cesàro averages as well as the first variance for both finite volume methods. For the empirical means of the corresponding Dirac distributions the convergence in the Wasserstein distance will be shown as well.

### 5.1 FLM finite volume method

We assume that the physical space is a polyhedral domain  $\Omega \subset R^d$ ,  $d = 2, 3$ , decomposed into compact polygonal sets (tetrahedral or parallelepipedal elements)

$$\bar{\Omega} = \bigcup_{K \in \mathcal{T}_h} K.$$

We denote by  $h$  the maximal size of the mesh,

$$h = \max_{K \in \mathcal{T}_h} h_K$$

with  $h_K$  being the diameter of an element  $K$ . The elements are sharing either a common face, edge, or vortex. We assume that the mesh  $\mathcal{T}_h$  satisfies the standard regularity assumptions, cf. [18, 22]. More precisely, let a parameter  $\theta_h$  be defined as

$$\theta_h = \inf \left\{ \frac{\xi_K}{h_K}, K \in \mathcal{T}_h \right\}, \quad (5.1)$$

where  $\xi_K$  stands for the diameter of the largest ball included in  $K$ . Then the mesh  $\mathcal{T}_h$  is said to be regular and quasi-uniform, if there exists positive real numbers  $c_0$  and  $\theta_0$  independent of  $h$  such that

$$\theta_h \geq \theta_0 \text{ and } c_0 h \leq h_K, \quad (5.2)$$

respectively.

The set of all faces is denoted by  $\Sigma_h$ , while  $\Sigma_h^{int} = \Sigma_h \setminus \partial\Omega$  stands for the set of all interior faces. Each face is associated with a normal vector  $\mathbf{n}$ . In what follows, we shall suppose

$$|K|_d \approx h^d, \quad |\sigma|_{d-1} \approx h^{d-1} \text{ for any } K \in \mathcal{T}_h, \sigma \in \Sigma.$$

Let us denote by  $\mathcal{P}_h^0$  a space of piecewise constant function on  $\mathcal{T}_h$ . For a function  $f_h \in \mathcal{P}_h^0$  we define

$$\begin{aligned} f_h^{\text{out}}(x) &= \lim_{\delta \rightarrow 0^+} f_h(x + \delta \mathbf{n}), & \overline{f_h} &= \frac{f_h^{\text{in}}(x) + f_h^{\text{out}}(x)}{2}, \\ f_h^{\text{in}}(x) &= \lim_{\delta \rightarrow 0^+} f_h(x - \delta \mathbf{n}), & [[f_h]] &= f_h^{\text{out}}(x) - f_h^{\text{in}}(x) \end{aligned}$$

whenever  $x \in \sigma \in \Sigma_h^{int}$ .

Finally, let  $D_t$  denote the first order backward finite difference approximating the time derivative, i.e.

$$D_t f_h(t) = \frac{f_h(t_{k+1}) - f_h(t_k)}{\Delta t}, \quad f_h(t_k), f_h(t_{k+1}) \in \mathcal{P}_h^0,$$

where  $\Delta t$  is a mesh step parameter on a time interval  $[0, T]$ ,  $t_k = k\Delta t$  and  $t \in (t_k, t_{k+1}]$ ,  $k = 1, 2, \dots$

The *numerical solutions* are piecewise constant functions on  $(0, T) \times \Omega$ , such that  $\varrho_h(t) \equiv \varrho_h(t_{k+1}) \in \mathcal{P}_h^0(\Omega_h)$ ,  $\mathbf{m}_h(t) \equiv \mathbf{m}_h(t_{k+1}) \in \mathcal{P}_h^0(\Omega_h; R^d)$ , and  $E_h(t) \equiv E_h(t_{k+1}) \in \mathcal{P}_h^0(\Omega_h)$ ,  $t \in (t_k, t_{k+1}]$  satisfying the following discrete equations:

- **Continuity equation**

$$\int_{\Omega_h} D_t \varrho_h \Phi \, dx - \sum_{\sigma \in \Sigma_h^{int}} \int_{\sigma} F_h(\varrho_h, \mathbf{u}_h) [[\Phi]] \, dS(x) = 0 \text{ for any } \Phi \in \mathcal{P}_h^0(\Omega_h), \quad (5.3)$$

where

$$\mathbf{u}_h = \frac{\mathbf{m}_h}{\varrho_h}.$$

- **Momentum equation**

$$\begin{aligned}
& \int_{\Omega_h} D_t \mathbf{m}_h \cdot \Phi \, dx - \sum_{\sigma \in \Sigma_h^{int}} \int_{\sigma} \mathbf{F}_h(\mathbf{m}_h, \mathbf{u}_h) \cdot [[\Phi]] \, dS(x) - \sum_{\sigma \in \Sigma_h^{int}} \int_{\sigma} \overline{p_h} \mathbf{n} \cdot [[\Phi]] \, dS(x) \\
& = -h^{\alpha-1} \sum_{\sigma \in \Sigma_h^{int}} \int_{\sigma} [[\mathbf{u}_h]] \cdot [[\Phi]] \, dS(x) \text{ for all } \Phi \in \mathcal{P}_h^0(\Omega_h, R^d),
\end{aligned} \tag{5.4}$$

where

$$p_h = (\gamma - 1) \left( E_h - \frac{1}{2} \frac{|\mathbf{m}_h|^2}{\varrho_h} \right).$$

- **Energy equation**

$$\begin{aligned}
& \int_{\Omega_h} D_t E_h \Phi \, dx - \sum_{\sigma \in \Sigma_h^{int}} \int_{\sigma} F_h(E_h, \mathbf{u}_h) [[\Phi]] \, dS(x) \\
& - \sum_{\sigma \in \Sigma_h^{int}} \int_{\sigma} \overline{p_h} [[\Phi \mathbf{u}_h]] \cdot \mathbf{n} \, dS(x) + \sum_{\sigma \in \Sigma_h^{int}} \int_{\sigma} \overline{p_h} \Phi [[\mathbf{u}_h]] \cdot \mathbf{n} \, dS(x) \\
& = -h^{\alpha-1} \sum_{\sigma \in \Sigma_h^{int}} \int_{\sigma} [[\mathbf{u}_h]] \cdot \overline{\mathbf{u}_h} [[\Phi]] \, dS(x) \text{ for all } \Phi \in \mathcal{P}_h^0(\Omega_h).
\end{aligned} \tag{5.5}$$

The function  $F_h$  stays for a *finite volume numerical flux* approximating the physical flux. In the literature one can find already a large variety of different numerical fluxes proposed for the hyperbolic conservation laws and the Euler equations in particular, see, e.g., [28, 29, 34, 40, 42, 43] and the references therein. In [25] we have used the following numerical flux function based on the upwinding strategy

$$F_h(r_h, \mathbf{u}_h) = Up[r_h, \mathbf{u}_h] - \mu_h [[r_h]], \quad r_h \in \mathcal{P}_h^0, \tag{5.6}$$

where  $\mu_h \geq 0$  and  $Up[r_h, \mathbf{u}_h]$  is a classical upwinding of  $r_h$ . This means that depending on the sign of the normal component of the velocity  $\overline{\mathbf{u}_h} \cdot \mathbf{n}$ ,  $r_h$  is taken to be either the upward or downward value of the neighbouring cells. More precisely, we have

$$Up[r_h, \mathbf{u}_h] = \overline{r_h} \overline{\mathbf{u}_h} \cdot \mathbf{n} - \frac{1}{2} |\overline{\mathbf{u}_h} \cdot \mathbf{n}| [[r_h]] = r_h^{\text{in}} [\overline{\mathbf{u}_h} \cdot \mathbf{n}]^+ + r_h^{\text{out}} [\overline{\mathbf{u}_h} \cdot \mathbf{n}]^-. \tag{5.7}$$

The numerical flux  $\mathbf{F}_h(\mathbf{m}_h, \mathbf{u}_h)$  denotes the corresponding vector-valued flux function for the approximation of a physical flux in the momentum equation. Note, that our upwinding  $Up[r_h, \mathbf{u}_h]$ ,  $r_h = \varrho_h, \mathbf{m}_h, E_h$ , is based only on the sign of the normal component of velocity, that is typically used in incompressible flow approximations, instead of the sign of the eigenvalues as it is standard in the flux-vector splitting schemes for compressible flows. Instead of the corresponding eigenvalues of the underlying hyperbolic system we add a numerical diffusion term  $-\mu_h [[r_h]]$  for the conservative variables. In numerical simulations one can take, for instance,  $h^\beta \lesssim \mu_h \lesssim 1$  with  $0 \leq \beta < 1$ .

### 5.1.1 Stability and consistency

The finite volume method (5.3)-(5.5) has the following remarkable properties that have been proven in [25].

- *Positivity of the discrete density and temperature:* numerical density and temperature remain strictly positive on any finite time interval.
- *Entropy stability:* discrete entropy inequality holds, cf. the concept of entropy stable numerical schemes [50, 51].
- *Minimum entropy principle:* the discrete entropy attains its minimum at the initial time.
- *Weak BV estimates:* discrete entropy inequality allows us to control suitable weak BV norms of the discrete density, temperature and velocity.

It is to be pointed out that the numerical diffusions  $\mu_h[[\varrho_h]]$ ,  $\mu_h[[\mathbf{m}_h]]$  and  $h^{\alpha-1}[[\mathbf{u}_h]]$ ,  $h^{\alpha-1}[[\mathbf{u}_h]]\overline{\mathbf{u}_h}$  arising from the numerical flux and additional  $h^\alpha$ -diffusive terms, respectively, allow us to prove *positivity of the discrete density* on each  $\mathcal{T}_h$ , i.e.

for any  $T > 0$ , there exists  $\underline{\varrho} = \underline{\varrho}(h, T) > 0$ , such that  $\varrho_h(t) \geq \underline{\varrho} > 0$  for all  $t \in [0, T]$ , if the initial data satisfy the corresponding condition.

Further, the minimum entropy principle yields the positivity of the discrete pressure and temperature, see [25]. Taking into account a priori estimates that yield uniform bounds on  $\varrho_h \in L^\infty((0, T), L^\gamma(\Omega_h))$ ,  $\mathbf{m}_h \in L^\infty((0, T), L^{\frac{2\gamma}{\gamma+1}}(\Omega_h))$ , and  $E_h \in L^\infty((0, T), L^1(\Omega_h))$  and the weak BV estimates resulting from the discrete entropy inequality, we obtain the following consistency result of the finite volume method (5.3)–(5.5), see Section 3 and [25].

**Proposition 5.1** (Consistency of the FLM finite volume method). *Assume that the initial data  $\varrho_{0,h}$ ,  $\mathbf{m}_{0,h}$ ,  $E_{0,h}$  satisfy*

$$\varrho_{0,h} \geq \underline{\varrho} > 0, \quad E_{0,h} - \frac{1}{2} \frac{|\mathbf{m}_{0,h}|^2}{\varrho_{0,h}} > 0.$$

*Let  $[\varrho_h, \mathbf{m}_h, E_h]$  be the unique solution of the finite volume method (5.3)–(5.5) on the time interval  $[0, T]$ . Then*

$$\left[ \int_{\Omega_h} \varrho_h \varphi \, dx \right]_{t=0}^{t=\tau} = \int_0^\tau \int_{\Omega_h} [\varrho_h \partial_t \varphi + \mathbf{m}_h \cdot \nabla_x \varphi] \, dx \, dt + \int_0^\tau e_{1,h}(t, \varphi) \, dt \quad (5.8)$$

*for any  $\varphi \in C^1([0, T] \times \overline{\Omega_h})$ ;*

$$\left[ \int_{\Omega_h} \mathbf{m}_h \varphi \, dx \right]_{t=0}^{t=\tau} = \int_0^\tau \int_{\Omega_h} \left[ \mathbf{m}_h \cdot \partial_t \varphi + \frac{\mathbf{m}_h \otimes \mathbf{m}_h}{\varrho_h} : \nabla_x \varphi + p_h \operatorname{div}_x \varphi \right] \, dx \, dt + \int_0^\tau e_{2,h}(t, \varphi) \, dt \quad (5.9)$$

for any  $\varphi \in C^1([0, T] \times \bar{\Omega}_h; R^d)$ ,  $\varphi \cdot \mathbf{n}|_{\Omega_h} = 0$ ;

$$\int_{\Omega_h} E_h(t) \, dx = \int_{\Omega_h} E_{0,h} \, dx; \quad (5.10)$$

$$\left[ \int_{\Omega_h} \varrho_h \chi(s_h) \varphi \, dx \right]_{t=0}^{t=\tau} \geq \int_0^\tau \int_{\Omega_h} [\varrho_h \chi(s_h) \partial_t \varphi + \chi(s_h) \mathbf{m}_h \cdot \nabla_x \varphi] \, dx \, dt + \int_0^\tau e_{3,h}(t, \varphi) \, dt \quad (5.11)$$

for any  $\varphi \in C^1([0, T] \times \bar{\Omega}_h)$ ,  $\varphi \geq 0$ , and any  $\chi$ ,

$\chi : R \rightarrow R$  a non-decreasing concave function,  $\chi(s) \leq \bar{\chi}$  for all  $s \in R$ .

If, in addition,

$$h^\beta \lesssim \mu_h \lesssim 1, \quad 0 \leq \beta < 1, \quad 0 < \alpha < \frac{4}{3}, \quad (5.12)$$

and

$$0 < \underline{\varrho} \leq \varrho_h(t), \quad \vartheta_h(t) \leq \bar{\vartheta} \text{ for all } t \in [0, T] \text{ uniformly for } h \rightarrow 0, \quad (5.13)$$

then

$$\|e_{j,h}(\cdot, \varphi)\|_{L^1(0,T)} \lesssim h^\delta \|\varphi\|_{C^1} \text{ for some } \delta > 0, \quad j = 1, 2, 3.$$

**Remark 5.2.** In the case of uniform rectangular/cubic elements the conclusion of Proposition 5.1 remains valid for  $0 \leq \mu_h \lesssim 1$ , and  $\varphi \in C^1([0, T]; C^2(\bar{\Omega}_h; R^d))$ ,  $\varphi \cdot \mathbf{n}|_{\Omega_h} = 0$ . Moreover, if  $d = 2$  then the condition (5.12) can be relaxed to  $0 \leq \beta < 1$ ,  $0 < \alpha < 2$ . Let us point out that omitting the artificial diffusion terms, i.e.  $\mu_h = 0$  and removing the terms with the factor  $h^{\alpha-1}$ , yields the upwind finite volume scheme.

Under the extra hypothesis (5.13), the numerical solutions  $\{\varrho_h, \mathbf{m}_h, S_h, E_h\}_{h \searrow 0}$  resulting from the scheme (5.3)–(5.5) represent a family of *admissible consistent approximate solutions* in the sense of Definition 2.1. In particular, the conclusion of Theorem 4.2 as well as other results obtained in Section 4 can be applied.

## 5.2 GRP finite volume method

The generalized Riemann problem finite volume method is one of successful standard numerical methods to simulate the Euler equations. It was developed as an analytical second order accurate extension of the classical Godunov finite volume method. Originally the method was based on the Lagrangian formulation [4, 5]. A direct Eulerian GRP scheme was presented in [6, 7, 45] by employing the regularity property of the Riemann invariants. Theoretically, a close coupling between the spatial and temporal evolution is recovered through the analysis of detailed wave interactions in the GRP scheme. The GRP method has been applied successfully to develop high resolution schemes and used for many engineering problems, see, e.g., [5, 13, 44] and the references therein.

To describe the main ingredients of the GRP finite volume method let us consider a two-dimensional regular rectangular grid with mesh cells  $K_{ij} \equiv [x_{i-1/2}, x_{i+1/2}] \times [y_{j-1/2}, y_{j+1/2}]$ ,  $x_{i\pm 1/2} = x_i \pm \Delta x/2$ ,  $y_{j\pm 1/2} = y_j \pm \Delta y/2$ ,  $\Delta x = h = \Delta y$ ,  $i, j \in \mathbb{N}$ . The basic idea of the GRP scheme consists of replacing the exact solution  $\mathbf{U} \equiv [\rho, \mathbf{m}, E]$  on a mesh cell  $K_{ij}$  by a piecewise linear function

$$\mathbf{U}(x, y, t) = \mathbf{U}(x_i, y_j, t) + \mathbf{U}_x(x_i, y_j, t)(x - x_i) + \mathbf{U}_y(x_i, y_j, t)(y - y_j), \quad (5.14)$$

and analytically solve locally at each cell interface  $\sigma \in \partial K_{ij}$  an one-dimensional generalized Riemann problem with the initial data

$$\mathbf{U}(\xi, t = 0) = \begin{cases} \mathbf{U}_L + \mathbf{U}'_L \xi, & \xi < 0 \\ \mathbf{U}_R + \mathbf{U}'_R \xi, & \xi > 0. \end{cases} \quad (5.15)$$

Let us now denote by  $\mathbf{F} = (\mathbf{F}_1, \mathbf{F}_2)$  the physical flux of the Euler equations (1.1), i.e.

$$\mathbf{F} = \left[ \mathbf{m}, \frac{\mathbf{m} \otimes \mathbf{m}}{\rho} + p\mathbb{I}, (E + p) \frac{\mathbf{m}}{\rho} \right].$$

Then the GRP numerical flux on the cell interface  $\sigma = (x_{i+1/2}, y)$ ,  $y \in [y_{j-1/2}, y_{j+1/2}]$ , is given as

$$\mathbf{F}_h \equiv \mathbf{F}_{i+1/2,j}^{k+1/2} = \mathbf{F} \left( \mathbf{U}_{i+1/2,j}^{k+1/2} \right), \quad \mathbf{U}_{i+1/2,j}^{k+1/2} = \mathbf{U}_{i+1/2,j}^k + \frac{\Delta t}{2} (\mathbf{U}_t)_{i+1/2,j}^k.$$

Here  $\mathbf{U}_{ij}^k$  is the cell average of  $\mathbf{U}(x, y, t_k)$  over the control volume  $K_{ij}$  evaluated at time  $t_k$ . The resulting scheme enjoys the second order accuracy both in space and time

$$\mathbf{U}_{ij}^{k+1} = \mathbf{U}_{ij}^k - \frac{\Delta t}{\Delta x} \left[ \mathbf{F}_{h,1} \left( \mathbf{U}_{i+1/2,j}^{k+1/2} \right) - \mathbf{F}_{h,1} \left( \mathbf{U}_{i-1/2,j}^{k+1/2} \right) \right] - \frac{\Delta t}{\Delta y} \left[ \mathbf{F}_{h,2} \left( \mathbf{U}_{i,j+1/2}^{k+1/2} \right) - \mathbf{F}_{h,2} \left( \mathbf{U}_{i,j-1/2}^{k+1/2} \right) \right]. \quad (5.16)$$

Gradients arising in (5.14) are standardly computed by the so-called minmod limiter to avoid spurious oscillations on discontinuities, see, e.g., [4].

### 5.3 Numerical experiments

In this section we consider two classical benchmarks, the Kelvin-Helmholtz and the Richtmyer-Meshkov problems, and illustrate robustness of the concept of  $\mathcal{K}$ -convergence using, as an example, the FLM (5.3)–(5.5) and GRP (5.16) finite volume schemes. These benchmarks have been also used by Fjordholm et al. [31, 32], where the *weak*(\*)-convergence of the statistical solutions has been investigated. It is to be pointed out that our theoretical results yield the *strong convergence* to a dissipative solution, which is the barycenter of the DMV solution. This fact will be confirmed by the numerical experiments in what follows.

For this purpose, we denote by  $E_1$ ,  $E_2$ ,  $E_3$ , and  $E_4$  the  $L^1$ -error of the difference between the numerical solution and the reference solution computed on a finest grid, the  $L^1$ -error of the Cesàro

averages, the  $L^1$ -error of the first variance, and the  $L^1$ -error of the Wasserstein distance<sup>1</sup> for the Cesàro average of the Dirac measures concentrated on numerical solutions, respectively. More precisely, we have

$$E_1 = \|U_{h_n} - U_{h_N}\|, \quad E_2 = \|\tilde{U}_{h_n} - \tilde{U}_{h_N}\|, \quad E_3 = \|U_{h_n}^\dagger - U_{h_N}^\dagger\|, \quad E_4 = \|W_1(\bar{\mathcal{V}}_{t,x}^n, \bar{\mathcal{V}}_{t,x}^N)\|,$$

where  $h_n = \frac{1}{n}$ ,  $n$  is the number of rectangular mesh cells in each direction,  $N = 2048$ ,  $\tilde{U}_{h_n} = \frac{1}{n} \sum_{j=1}^n U_{h_j}$ ,  $U_{h_n}^\dagger = \frac{1}{n} \sum_{j=1}^n |U_{h_j} - \tilde{U}_{h_n}|$ , and  $U \in \{\varrho, \mathbf{m}, S, E\}$ . In all of the following tests we set  $\Omega = [0, 1]^2$  and apply periodic boundary conditions.

**Experiment 1.** The first experiment is the Kelvin-Helmholtz problem [36, 38] with the initial data

$$(\varrho, u_1, u_2, p)(x) = \begin{cases} (2, -0.5, 0, 2.5), & \text{if } I_1 < x_2 < I_2 \\ (1, 0.5, 0, 2.5), & \text{otherwise.} \end{cases}$$

Here the interface profiles

$$I_j = I_j(x, \omega) := J_j + \epsilon Y_j(x, \omega), \quad j = 1, 2,$$

are chosen to be small perturbations around the lower  $J_1 = 0.25$  and the upper  $J_2 = 0.75$  interface, respectively. Further,

$$Y_j(x, \omega) = \sum_{n=1}^m a_j^n(\omega) \cos(b_j^n(\omega) + 2n\pi x_1), \quad j = 1, 2,$$

where  $a_j^n = a_j^n(\omega) \in [0, 1]$  and  $b_j^n = b_j^n(\omega) \in [-\pi, \pi]$ ,  $i = 1, 2$ ,  $n = 1, \dots, m$  are (fixed) random numbers. The coefficients  $a_j^n$  have been normalized such that  $\sum_{n=1}^m a_j^n = 1$  to guarantee that  $|I_j(x, \omega) - J_j| \leq \epsilon$  for  $j = 1, 2$ . We have set  $m = 10$  and  $\epsilon = 0.01$ .

In what follows we present the numerical simulations obtained by the FLM finite volume method with  $\alpha = 1.8$ ,  $\beta = 0.8$ , upwind finite volume method (see Remark 5.2) and the GRP finite volume method at the final time  $T = 2$ . It is the time when small-scales vortex sheets have already been formed at the interfaces.

In Table 1 we show the results of the convergence study for the errors  $E_1, \dots, E_4$  in density. We can clearly observe that none of the methods converges in the classical sense, i.e. single numerical solutions do not converge, see the first column. This behaviour is also demonstrated in the Figures 1, 2. Similar non-convergence results have been presented for the second order TeCNO scheme in [30].

The second, third and fourth columns in Table 1 show the convergence results for the Cesàro averages of numerical solutions and their first variance, as well as  $\mathcal{K}$ -convergence of the Wasserstein

---

<sup>1</sup>An open source library SciPy [37] was used to compute  $W_1$ -distance. We thank S. Mishra and K. Lye for pointing us this package.

distance of the corresponding Dirac measures. We should point out that the convergence is strong in the  $L^1$ -norm as proved above, cf. (4.3), (4.11)–(4.13) and Theorem 4.2. The graphs in Figure 1 show the results of the convergence study for all variables  $\rho, m, S, E$ . As expected, these variables behave in a similar manner.

Approximate solutions for the density computed by the second order GRP scheme are presented in Figure 2, which also clearly indicates that by refining the mesh we recover finer and finer vortex structures and the method does not converge in the classical sense. However, as already pointed out we have  $\mathcal{K}$ -convergence of the numerical solution and its first variance, see Figures 3, 4. The results obtained by the FLM scheme are similar, but more diffusive due to the first order accuracy and we do not present them here.

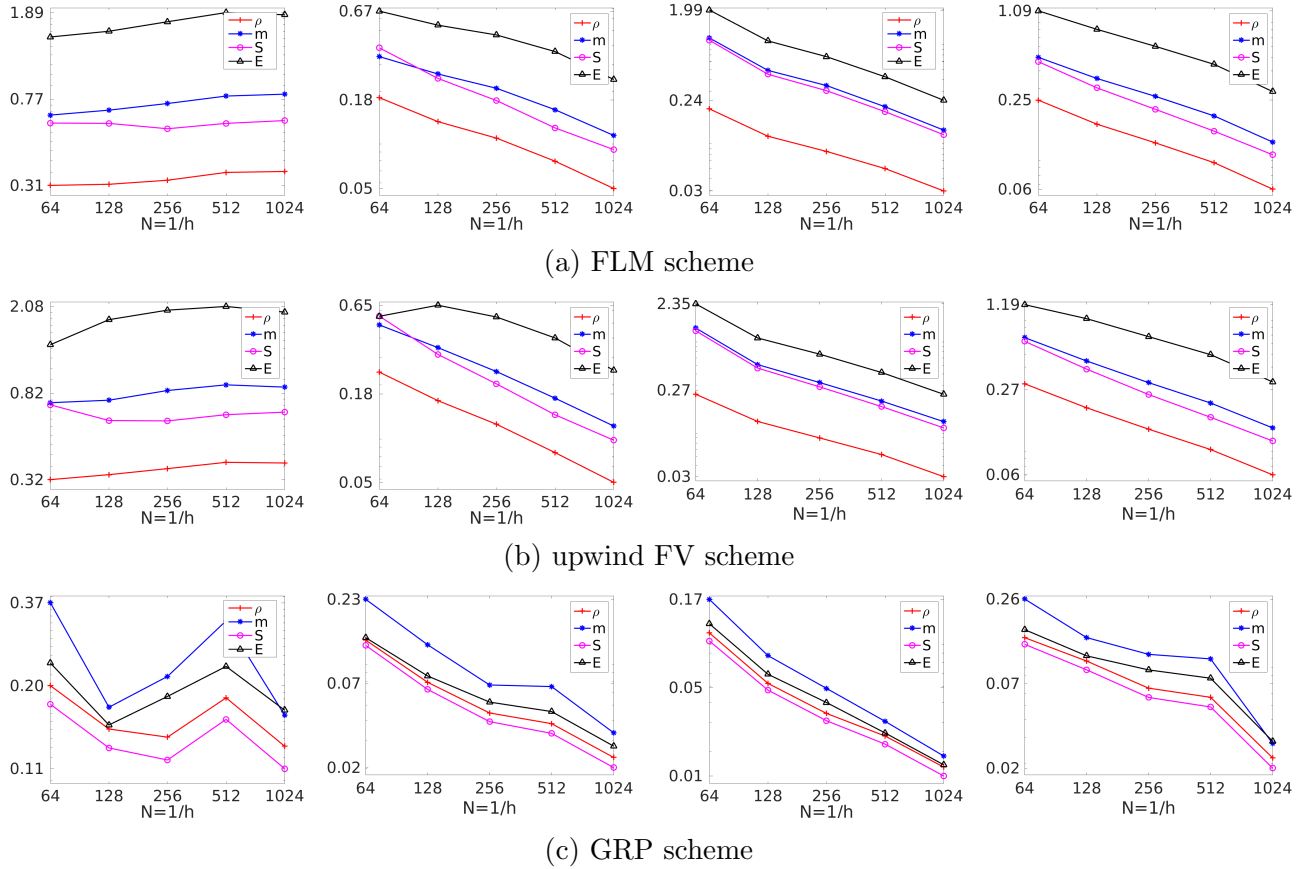


Figure 1: Experiment 1, convergence study for the Kelvin-Helmholtz problem:  $E_1, E_2, E_3,$  and  $E_4$  errors (left to right).



Table 1: Experiment 1, convergence study for the Kelvin-Helmholtz problem:  $E_1$ ,  $E_2$ ,  $E_3$ , and  $E_4$  errors for density (left to right).

mesh density	$E_1$		$E_2$		$E_3$		$E_4$	
	error	order	error	order	error	order	error	order
(a) FLM scheme								
64	3.09e-01	-	1.81e-01	-	2.00e-01	-	2.45e-01	-
128	3.13e-01	-0.02	1.26e-01	0.52	1.06e-01	0.92	1.64e-01	0.58
256	3.27e-01	-0.06	9.83e-02	0.36	7.44e-02	0.51	1.20e-01	0.45
512	3.54e-01	-0.12	6.94e-02	0.50	4.99e-02	0.58	8.62e-02	0.48
1024	3.58e-01	-0.01	4.59e-02	0.59	2.97e-02	0.75	5.54e-02	0.64
(b) upwind FV scheme								
64	3.24e-01	-	2.41e-01	-	2.40e-01	-	2.97e-01	-
128	3.41e-01	-0.08	1.59e-01	0.61	1.21e-01	0.99	1.95e-01	0.61
256	3.64e-01	-0.09	1.12e-01	0.50	7.96e-02	0.60	1.34e-01	0.54
512	3.90e-01	-0.10	7.36e-02	0.60	5.23e-02	0.61	9.37e-02	0.52
1024	3.87e-01	0.01	4.75e-02	0.63	3.00e-02	0.80	6.02e-02	0.64
(c) GRP scheme								
64	2.03e-01	-	1.28e-01	-	1.06e-01	-	1.44e-01	-
128	1.49e-01	0.45	6.95e-02	0.88	5.21e-02	1.03	9.98e-02	0.53
256	1.40e-01	0.08	4.45e-02	0.64	3.41e-02	0.61	6.52e-02	0.61
512	1.86e-01	-0.41	3.81e-02	0.22	2.48e-02	0.46	5.65e-02	0.21
1024	1.31e-01	0.50	2.33e-02	0.71	1.60e-02	0.63	2.18e-02	1.37

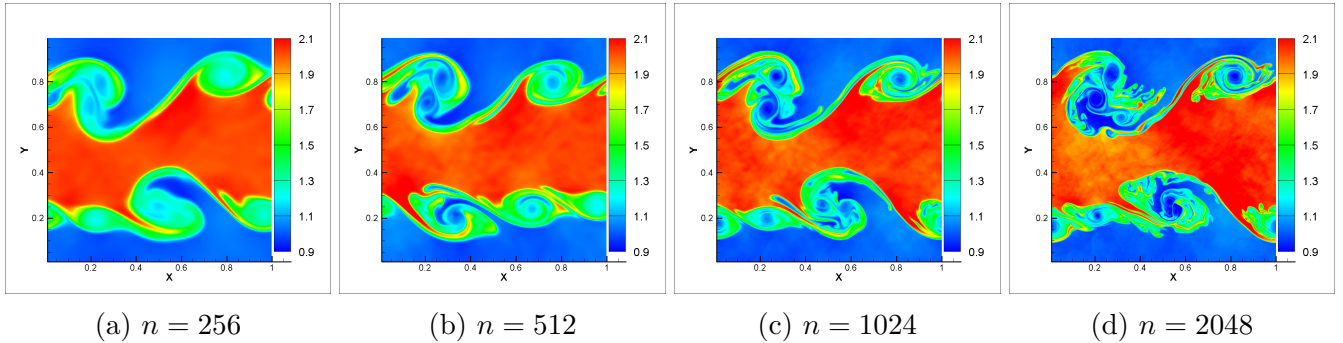


Figure 2: Experiment 1, density computed by the GRP scheme at  $T = 2$  for the Kelvin-Helmholtz problem on a mesh with  $n \times n$  cells.

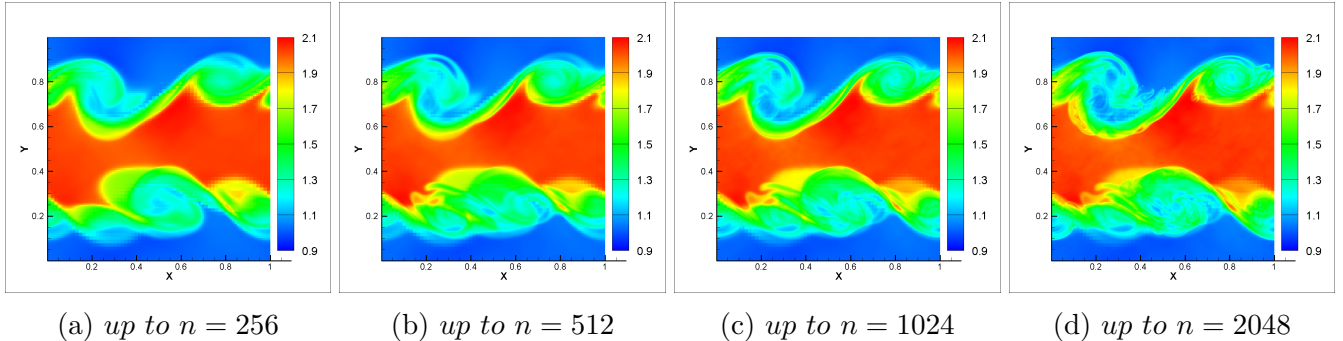


Figure 3: Experiment 1, Cesàro averages of the density computed by the GRP method on meshes with  $j \times j$  cells,  $j = 64, 128, \dots, n$ , for the Kelvin-Helmholtz problem.

**Experiment 2.** The second experiment is the Richtmyer-Meshkov problem [46, 48] of complex interaction of strong shocks with unstable interfaces. The initial data are given as

$$u_1 = u_2 = 0, \quad p(x) = \begin{cases} 20, & \text{if } r < 0.1, \\ 1, & \text{otherwise,} \end{cases} \quad \rho(\mathbf{x}) = \begin{cases} 2, & \text{if } r < I(x, \omega), \\ 1, & \text{otherwise,} \end{cases}$$

where  $r = \sqrt{(x_1 - 0.5)^2 + (x_2 - 0.5)^2}$  and the radial density interface  $I(x, \omega) = 0.25 + 0.01Y(x, \omega)$  is perturbed by

$$Y(x, \omega) = \sum_{n=1}^m a^n(\omega) \cos(\phi + b^n(\omega)).$$

Here  $\phi = \arccos(x_2/r)$ , and the parameters  $a^n, b^n$  are random data chosen in the same way as in Experiment 1. We have computed numerical solutions by the FLM, upwind FV and GRP schemes until the final time  $T = 4$ . At this time the leading shock waves re-entered from the corners due to the periodic boundary conditions and interact with each others leading to complex small-scales vortices.

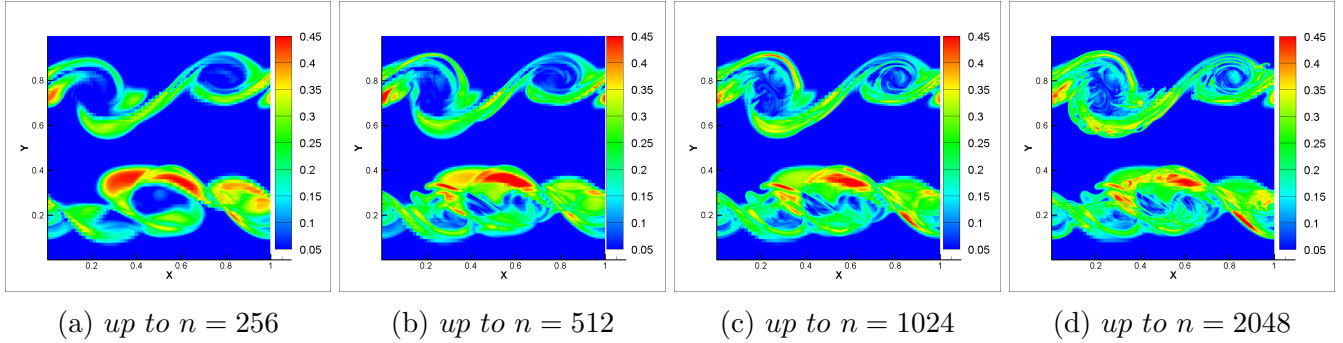


Figure 4: Experiment 1, first variance of the density computed by the GRP method on meshes with  $j \times j$  cells,  $j = 64, 128, \dots, n$ , for the Kelvin-Helmholtz problem.

Table 2 and Figure 5 demonstrate that there is no convergence of single numerical solutions in the classical sense, see the first column, but we have  $L^1$ -convergence of the Cesàro averages of numerical solutions and their first variance as well as  $\mathcal{K}$ -convergence of the Wasserstein distance of the corresponding Dirac distributions. Numerical approximation of the density, its Cesàro averages and of the first variance at time  $T = 4$  is illustrated by Figures 6–8. We can again confirm that single numerical solutions do not converge in the classical sense, but we have  $\mathcal{K}$ -convergence that is strong in  $L^1(\Omega)$ .

Let us point out that in both experiments convergence of the Cesàro averages of numerical solutions and their first variance as well as  $\mathcal{K}$ -convergence of the corresponding Dirac distributions is approximately of order 0.5.

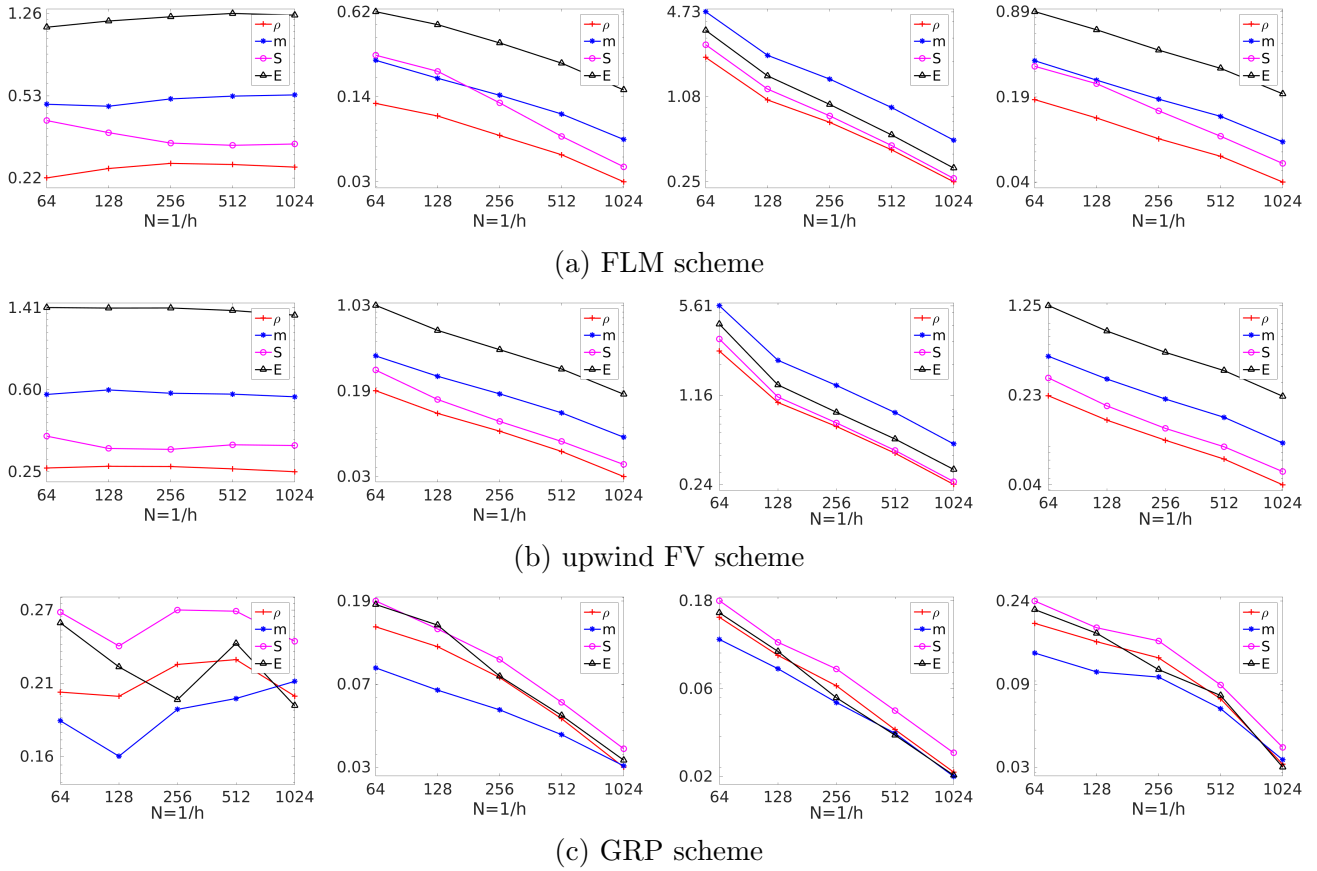


Figure 5: Experiment 2, convergence study for the Richtmyer-Meshkov problem:  $E_1, E_2, E_3$  and  $E_4$  errors (left to right).

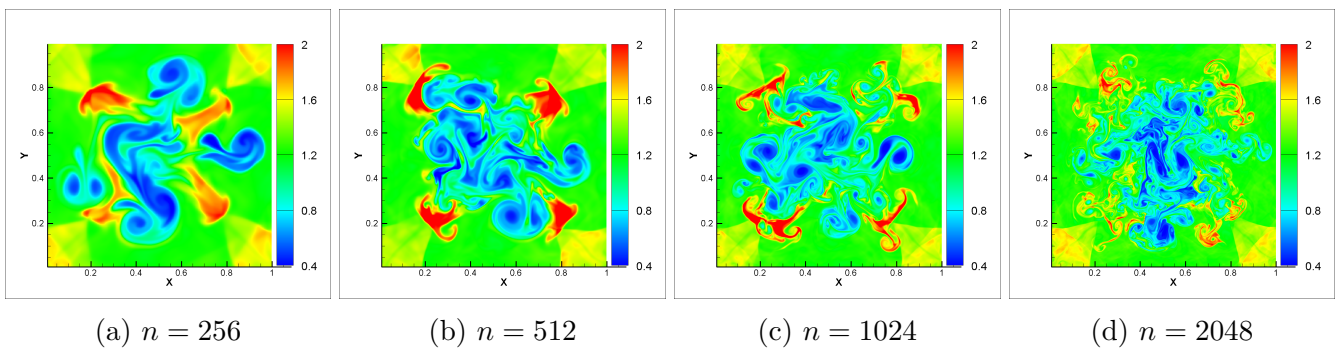
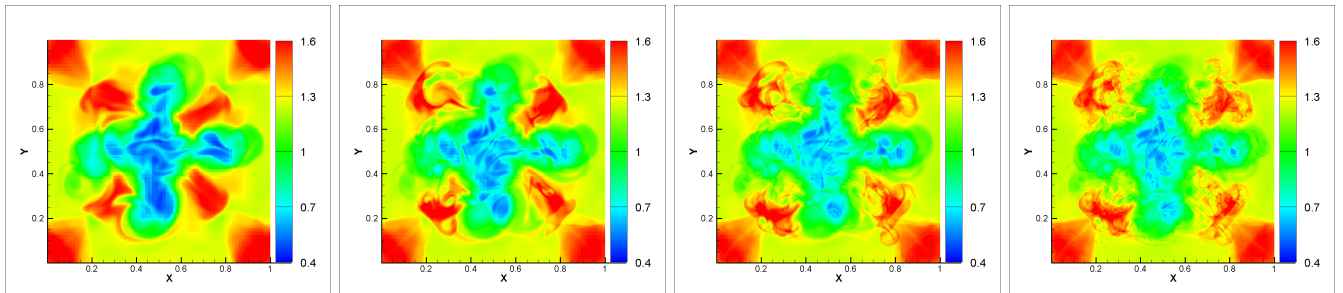


Figure 6: Experiment 2, density computed by the GRP scheme at  $T = 4$  for the Richtmyer-Meshkov problem on a mesh with  $n \times n$  cells.

Table 2: Experiment 2, convergence study for the Richtmyer-Meshkov problem:  $E_1, E_2, E_3$  and  $E_4$  errors for density (left to right).

mesh density	$E_1$		$E_2$		$E_3$		$E_4$		
	error	order	error	order	error	order	error	order	
(a) FLM scheme									
64	2.19e-01	-	1.27e-01	-	2.14e+00	-	1.80e-01	-	
128	2.42e-01	-0.14	1.02e-01	0.32	1.02e+00	1.07	1.29e-01	0.48	
256	2.56e-01	-0.08	7.25e-02	0.49	6.93e-01	0.56	8.86e-02	0.54	
512	2.53e-01	0.02	5.19e-02	0.48	4.30e-01	0.69	6.45e-02	0.46	
1024	2.46e-01	0.04	3.25e-02	0.68	2.47e-01	0.80	4.05e-02	0.67	
(b) upwind FV scheme									
64	2.65e-01	-	1.86e-01	-	2.53e+00	-	2.32e-01	-	
128	2.70e-01	-0.03	1.18e-01	0.66	1.02e+00	1.31	1.47e-01	0.66	
256	2.69e-01	0.00	8.28e-02	0.51	6.69e-01	0.61	1.01e-01	0.54	
512	2.63e-01	0.03	5.52e-02	0.59	4.18e-01	0.68	7.11e-02	0.51	
1024	2.55e-01	0.04	3.34e-02	0.72	2.41e-01	0.79	4.40e-02	0.69	
(c) GRP scheme									
64	2.01e-01	-	1.41e-01	-	1.44e-01	-	1.80e-01	-	
128	1.98e-01	0.02	1.11e-01	0.35	8.71e-02	0.72	1.44e-01	0.32	
256	2.23e-01	-0.17	7.61e-02	0.54	5.83e-02	0.58	1.19e-01	0.28	
512	2.27e-01	-0.03	4.62e-02	0.72	3.27e-02	0.83	7.26e-02	0.71	
1024	1.98e-01	0.20	2.57e-02	0.85	1.87e-02	0.81	3.30e-02	1.14	



(a) up to  $n = 256$

(b) up to  $n = 512$

(c) up to  $n = 1024$

(d) up to  $n = 2048$

Figure 7: Experiment 2, Cesàro averages of the density computed by the GRP method on meshes with  $j \times j$  cells,  $j = 64, 128, \dots, n$ , for the Richtmyer-Meshkov problem.

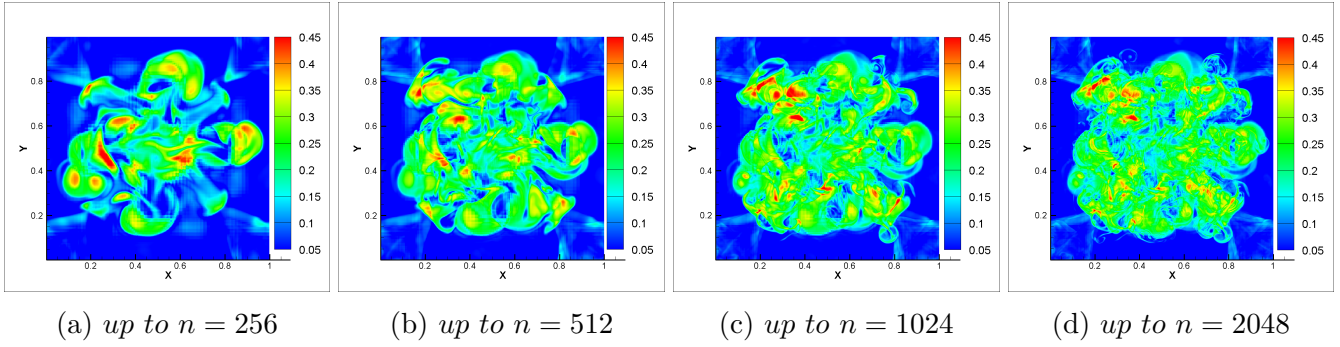


Figure 8: Experiment 2, first variance of the density computed by the GRP method on meshes with  $j \times j$  cells,  $j = 64, 128, \dots, n$ , for the Richtmyer-Meshkov problem.

## 6 Conclusion

We have developed a new strategy for computing dissipative measure-valued (DMV) solutions of the Euler system of gas dynamics. It is a well-known fact that the Euler equations in two- and three-space dimensions are essentially ill-posed, which is demonstrated by the fact that infinitely many admissible weak solutions exist even for smooth initial data. Therefore the question of the convergence of numerical schemes, which is studied in the present paper, is of fundamental importance.

We have introduced the concept of consistent approximations and showed that they generate DMV solutions, see Section 2. An example of such a consistent approximation is the FLM finite volume method developed in [25], see Section 5. We have also presented an interesting property, that can be seen as a sharper version of the Lax-Wendroff theorem: a consistent numerical approximations converge either strongly or their (weak) limit is not a weak solution of the Euler system, see Section 3.

In view of these facts a suitable concept of generalized solutions of the Euler system is inevitable. Applying  $\mathcal{K}$ -convergence to the Dirac distributions concentrated on the numerical solutions we showed in Section 4 that a limiting DMV solution can be effectively computed by the Cesàro averages of the consistent approximations. To this goal, we have studied the convergence of observable quantities, such as the expected value and the first variance, see (4.2), (4.3), (4.11), (4.12), (4.13), and showed that the density, momentum and the entropy converge strongly in  $L^q((0, T) \times \Omega)$  for some  $q \geq 1$ . Note that the energy converges a.e. in  $(0, T) \times \Omega$ .

As an added benefit, we have also obtained that the Cesàro averages of the Dirac distributions converge in the Wasserstein distance  $W_q$  and strongly in  $L^q((0, T) \times \Omega)$ , for some  $q \geq 1$ , see Theorem 4.2.

In Section 5 we have described two numerical schemes for the Euler equations, the FLM finite volume method [25] and the standard second order GRP method [5–7]. Both methods confirm our theoretical results on  $\mathcal{K}$ -convergence. This is demonstrated in Section 5.3, where we solve numerically two well-known benchmarks, the Kelvin-Helmholtz and the Richtmyer-Meshkov instability problems. As expected, single solutions computed by both methods do not converge due to new fine scale structures arising on refined meshes. On the other hand, we have demonstrated  $\mathcal{K}$ -convergence of the corresponding Dirac distributions as well as the strong convergence of Cesàro averages of the numerical solutions and their first variance.

$\mathcal{K}$ -convergence can be seen as a new tool in numerical analysis of ill-posed partial differential equations. In particular, it can be applied to other well-established numerical schemes for the Euler equations in order to study their convergence. In future it will be interesting to extend the concept of dissipative measure-valued solutions and  $\mathcal{K}$ -convergence to general hyperbolic conservation laws.

## References

- [1] E.J. Balder. Lectures on Young measure theory and its applications in economics. *Rend. Istit. Mat. Univ. Trieste*, 31(suppl. 1):1–69, 2000. Workshop on Measure Theory and Real Analysis (Italian) (Grado, 1997).
- [2] E.J. Balder. On Prokhorov’s theorem for transition probabilities. *Sém. Anal. Convexe*, **19**, 9.1–9.11, 1989.
- [3] J.M. Ball. A version of the fundamental theorem for Young measures. *In Lect. Notes in Physics 344, Springer-Verlag*, pages 207–215, 1989.
- [4] M. Ben-Artzi and J. Falcovitz. A second-order Godunov-type scheme for compressible fluid dynamics. *J. Comput. Phys.*, **55**:1–32, 1984.
- [5] M. Ben-Artzi and J. Falcovitz. *Generalized Riemann Problems in Computational Fluid Dynamics*. Cambridge University Press, 2003.
- [6] M. Ben-Artzi, J. Li and G. Warnecke. A direct Eulerian GRP scheme for compressible fluid flows. *J. Comput. Phys.*, **218**:19–34, 2006.
- [7] M. Ben-Artzi and J. Li. Hyperbolic balance laws: Riemann invariants and the generalized Riemann problem. *Numer. Math.*, **106(3)**: 369–425, 2007.
- [8] D. Breit, E. Feireisl, and M. Hofmanová. Dissipative solutions and semiflow selection for the complete Euler system. Preprint arXiv:1904.00622, submitted, 2019.
- [9] H. Brenner. Fluid mechanics revisited. *Phys. A*, **349**:190–224, 2006.
- [10] J. Březina, E. Feireisl. Measure-valued solutions to the complete Euler system. *J. Math. Soc. Jpn.* **70(4)**: 1227-1245, 2018.
- [11] Ch. Castaing, P.R. de Fitte, and M. Valadier. *Young Measures on Topological Spaces*. Springer, 2004.
- [12] N. Chaudhuri. Asymptotic limit of consistent approximations to the full Euler system. in preparation, 2019.
- [13] J. Cheng, Z. Du, X. Lei, Y. Wang, J. Li. A two-stage fourth-order discontinuous Galerkin method based on the GRP solver for the compressible Euler equations. *Computers & Fluids*, **181**:248–258, 2019.
- [14] E. Chiodaroli. A counterexample to well-posedness of entropy solutions to the compressible Euler system. *J. Hyperbolic Differ. Equ.*, **11(3)**:493–519, 2014.



- [15] E. Chiodaroli, C. De Lellis, and O. Kreml. Global ill-posedness of the isentropic system of gas dynamics. *Comm. Pure Appl. Math.*, **68**(7):1157–1190, 2015.
- [16] E. Chiodaroli and O. Kreml. On the energy dissipation rate of solutions to the compressible isentropic Euler system. *Arch. Ration. Mech. Anal.*, **214**(3):1019–1049, 2014.
- [17] E. Chiodaroli, O. Kreml, V. Mácha, and S. Schwarzacher. Nonuniqueness of admissible weak solutions to the compressible Euler equations with smooth initial data. *Arxiv Preprint Series*, **arXiv 1812.09917v1**, 2019.
- [18] P.G. Ciarlet. *The Finite Element Method for Elliptic Problems*. Classics in Applied Mathematics, Society for Industrial and Applied Mathematics, 2002.
- [19] C. De Lellis, L. Székelyhidi, Jr. On admissibility criteria for weak solutions of the Euler equations. *Arch. Ration. Mech. Anal.* **195**(1): 225–260, 2010.
- [20] R. DiPerna, A. Majda. Oscillations and concentrations in weak solutions of the incompressible fluid equations. *Commun. Math. Phys.* **108**(4): 667–689, 1987.
- [21] V. Elling. A possible counterexample to well posedness of entropy solutions and Godunov scheme convergence. *Math. Comp.* **75**(256): 1721–1733, 2006.
- [22] R. Eymard, T. Gallouët, and R. Herbin. Finite volume methods. *Handbook of numerical analysis 7*: 713–1018, 2000.
- [23] E. Feireisl, P. Gwiazda, A. Świerczewska-Gwiazda, and E. Wiedemann. Dissipative measure-valued solutions to the compressible Navier–Stokes system. *Calc. Var. Partial Diff.* **55**(6): 55–141, 2016.
- [24] E. Feireisl, M. Hofmanová On the vanishing viscosity limit of the isentropic Navier-Stokes system, *Arxiv Preprint Series*, **arXiv 1905.02548**, 2019.
- [25] E. Feireisl, M. Lukáčová-Medvidřová, and H. Mizerová. A finite volume scheme for the Euler system inspired by the two velocities approach. Preprint arXiv:1805.05072, submitted, 2018.
- [26] E. Feireisl, M. Lukáčová-Medvidřová, H. Mizerová, and B. She. On the convergence of a finite volume method for the Navier-Stokes-Fourier system. Preprint arXiv:1903.08526, submitted, 2019.
- [27] E. Feireisl, C. Klingenberg, O. Kreml, and S. Markfelder. On oscillatory solutions to the complete Euler system. Preprint arXiv:1710.10918, submitted, 2017.
- [28] M. Feistauer. *Mathematical Methods in Fluid Dynamics*. Pitman Monographs and Surveys in Pure and Applied Mathematics Series 67, Longman Scientific & Technical, Harlow, 1993.

- [29] M. Feistauer, J. Felcman, and I. Straškraba. *Mathematical and Computational Methods for Compressible Flow*. Clarendon Press, Oxford, 2003.
- [30] U.S. Fjordholm, R. Käppeli, S. Mishra, and E. Tadmor. Construction of approximate entropy measure valued solutions for hyperbolic systems of conservation laws. *Found. Comp. Math.*, pages 1–65, 2015.
- [31] U. S. Fjordholm, S. Mishra, and E. Tadmor. On the computation of measure-valued solutions. *Acta Numer.* **25**: 567–679, 2016.
- [32] U.S. Fjordholm, K. Lye, S. Mishra, and F. Weber. Statistical solutions of hyperbolic systems of conservation laws: numerical approximation. Preprint arXiv:1906.02536, 2019.
- [33] U.S. Fjordholm, S. Solem. Second-order convergence of monotone schemes for conservation laws. *SIAM J. Numer. Anal.*, **54**(3):1920–1945, 2016.
- [34] E. Godlewski, P.-A. Raviart. *Numerical Approximation of Hyperbolic Systems of Conservation Laws*. Springer, 1996.
- [35] J.L. Guermond, B. Popov. Viscous regularization of the Euler equations and entropy principles. *SIAM J. Appl. Math.* **74**(2): 284–305, 2014.
- [36] H. von Helmholtz. On the discontinuous movements of fluids. *Monatsberichte der Königlichen Preussische Akademie der Wissenschaften zu Berlin* **23**: 215–278, 1868.
- [37] E. Jones, T. Oliphant, P. Peterson, et al. SciPy: Open source scientific tools for Python, 2001.
- [38] W.T. Kelvin. Hydrokinetic solutions and observations. *Philosophical Magazine* **42**: 362–377, 1871.
- [39] J. Komlós. A generalization of a problem of Steinhaus. *Acta Math. Acad. Sci. Hungar.* **18**:217–229, 1967.
- [40] D. Kröner. *Numerical Schemes for Conservation Laws*. Wiley-Teubner, 1997.
- [41] P. Lax, B. Wendroff. Systems of conservation laws. *Comm. Pure Appl. Math.* **8**: 217–237, 1960.
- [42] R.J. LeVeque. *Numerical Methods for Conservation Laws*. Lectures in Mathematics, ETH-Zürich Birkhäuser, 1990.
- [43] R.J. LeVeque. *Finite Volume Methods for Hyperbolic Problems*. Cambridge University Press, 2002.

- [44] J. Li and Z. Du. Two-stage fourth order time-accurate discretization for Lax–Wendroff type flow solvers I. Hyperbolic conservation laws. *SIAM J. Sci. Com.* **38 (5)**:3046–3068, 2016.
- [45] J. Li and Z. Sun. Remark on the generalized Riemann problem method for compressible fluid flows. *J. Comput. Phys.* **222(2)**:796–808, 2007.
- [46] E.E. Meshkov. Instability of the interface of two gases accelerated by a shock wave. *Soviet Fluid Dynamics* **4(5)**: 101–104, 1969.
- [47] P. Pedregal. *Parametrized Measures and Variational Principles*. Birkhäuser, Basel, 1997.
- [48] R.D. Richtmyer. Taylor instability in a shock acceleration of compressible fluids. *Comm. Pure Appl. Math.* **13(2)**: 297–319, 1960.
- [49] A. M. Ruf, E. Sande, and S. Solem. The optimal convergence rate of monotone schemes for conservation laws in the Wasserstein distance. *J. Sci. Comput.*, 2019.
- [50] E. Tadmor. Entropy stability theory for difference approximations of nonlinear conservation laws and related time dependent problems. *Acta Numer.* **12**: 451–512, 2003.
- [51] E. Tadmor. Minimum entropy principle in the gas dynamic equations. *Appl. Num. Math.* **2**: 211–219, 1986.
- [52] C. Villani. *Optimal Transport: old and new*. Springer, 2009.